JOINT INSTITUTE FOR NUCLEAR RESEARCH

Dzhelepov Laboratory of nuclear problems

FINAL REPORT ON THE START PROGRAMME

"*Radiation protection and the safety of radiation sources*"

Supervisor:

Prof. Dr. S. Abdelshakour

Joint Institute for Nuclear Research

Student:

Abdelrahman Ahmed Abdelaziz Mohamed

The Fayoum University in Egypt

Participation period:

Feb 15 - Mar 28

Winter Session 2026

Dubna, 2026

Table of Contents

Abstract

This study investigates the performance and optimization of radiation detection systems for gamma-ray and alpha-particle measurements, with emphasis on their applications in radiation safety and spectroscopy. The experimental work focuses on the evaluation of semiconductor detectors, including Cadmium Telluride (CdTe), Silicon (Si), and Gallium Arsenide (GaAs), in terms of energy calibration and detection efficiency using standard radioactive sources such as Cs-137, Co-57, Co-60, and Am-241.

In addition, scintillation detectors, namely Lanthanum Bromide ($LaBr_3$) and Bismuth Germinate (BGO), were analyzed to assess their energy resolution and response under varying applied voltages. The study also incorporates pixel detector measurements to determine the range of alpha particles in air, supported by Monte Carlo simulations using SRIM for validation and comparison.

Furthermore, X-ray spectrum simulations using a CdTe detector were performed to examine detector response at different energy levels and operating conditions, and were compared with experimental measurements to validate the detector model. The results demonstrate that increasing the applied voltage improves the energy resolution of scintillation detectors due to enhanced signal-to-noise ratio.

Overall, this work highlights the importance of detector material properties, operating conditions, and computational tools such as ROOT and Python in achieving accurate radiation measurements and optimizing detector performance. These findings demonstrate the practical significance of optimizing detector performance for reliable radiation measurements in both research and applied environments. The comparative analysis of different detector technologies provides a clear framework for selecting appropriate systems based on energy range, resolution requirements, and operational conditions. Such optimization is essential for improving measurement accuracy, enhancing radiation safety practices, and supporting the development of advanced detection systems in nuclear and medical physics applications.

Introduction

Radiation represents a fundamental mechanism of energy transfer that propagates through space and matter, playing a vital role in numerous scientific, industrial, and medical applications. It is broadly classified into two principal categories: ionizing and non-ionizing radiation. Ionizing radiation, which includes alpha particles, beta particles, gamma rays, X-rays, and neutrons, possesses sufficient energy to remove tightly bound electrons from atoms, resulting in ionization. This process can significantly alter chemical structures and may cause biological damage to living tissues. In contrast, non-ionizing radiation such as ultraviolet (UV) radiation, visible light, infrared radiation, and radio waves does not carry enough energy to ionize atoms, but instead interacts with matter primarily through excitation and thermal effects. Understanding the characteristics and interactions of these different types of radiation is essential for maximizing their beneficial applications while minimizing potential hazards.

In the medical field, ionizing radiation has become an indispensable tool for both diagnostic and therapeutic purposes. Diagnostic imaging techniques, including X-ray radiography, computed tomography (CT), and positron emission tomography (PET), rely on ionizing radiation to produce detailed images of internal anatomical structures, enabling accurate diagnosis of various diseases. Additionally, radiation therapy is widely used in oncology to destroy malignant cells while minimizing damage to surrounding healthy tissues. Despite these significant benefits, exposure to ionizing radiation carries inherent risks, such as radiation-induced tissue damage and an increased probability of cancer following excessive or prolonged exposure. Therefore, the implementation of effective radiation protection strategies is essential. The fundamental principle of radiation protection is to achieve the required clinical outcome while maintaining radiation exposure at the lowest possible level, thereby reducing both deterministic effects, such as tissue damage, and stochastic effects, such as cancer induction.

The advancement of radiation detection technology plays a crucial role in improving radiation protection and enhancing the accuracy of medical imaging systems. Radiation detectors are specialized instruments designed to identify and measure various properties of nuclear radiation, including energy, interaction time, spatial distribution, and particle type. Several categories of detectors are commonly

employed in radiation measurements, including semiconductor detectors, scintillation detectors, and gas-filled detectors. Among these, semiconductor detectors have gained significant importance due to their excellent energy resolution, high detection efficiency, and compact design.

In this study, the performance and registration efficiency of several semiconductor detectors namely Cadmium Telluride (CdTe), Silicon (Si), and Gallium Arsenide (GaAs) are investigated and compared. These detectors are widely utilized in radiation spectroscopy and dosimetry because of their capability to provide accurate energy measurements. To evaluate their spectroscopic characteristics, energy calibration and detector response analyses are performed using a set of standard radioactive sources, including Cs-137, Co-57, Co-60, and Am-241.

Furthermore, scintillation detectors such as Bismuth Germanate (BGO) and Lanthanum Bromide ($LaBr_3$) have demonstrated excellent performance in radiation monitoring and medical imaging applications. These detectors are characterized by high density and efficient conversion of incident radiation into visible photons, which enables accurate radiation measurement and high-resolution imaging. In addition, modern pixel detector technologies provide enhanced spatial resolution and enable detailed particle tracking at microscopic levels. Such capabilities are particularly important in advanced radiation measurements and in improving the early detection and analysis of tumor development.

Overall, continuous advancements in radiation detection systems contribute significantly to improving radiation safety, optimizing medical imaging techniques, and enhancing the accuracy of radiation measurements in both research and clinical applications.

1. Semiconductor detectors

Cadmium Telluride (CdTe) Detector

The Cadmium Telluride (CdTe) detector, particularly the X-123-CdTe model, is widely used for the detection of medium- to high-energy X-rays and gamma rays, typically above 30 keV. This detector system integrates several essential components, including the radiation detector itself, a power supply, an interface module, a preamplifier, and a digital pulse processing unit. Such integrated systems are commonly applied in various fields such as medical imaging, radiology, mammography, and the monitoring of radioactive materials including uranium and plutonium.

One of the major advantages of CdTe detectors is their high detection efficiency for characteristic X-rays. The detector can achieve nearly 100% efficiency for characteristic X-rays with energies up to approximately 100 keV. In contrast, silicon detectors with a thickness of about 0.5 mm tend to experience a significant reduction in sensitivity for photon energies exceeding approximately 15 keV. Due to these properties, CdTe detectors are particularly suitable for X-ray fluorescence (XRF) applications, especially in the analysis of high-atomic-number (high-Z) elements such as rare earth metals, lead, and mercury. They are also frequently utilized in the characterization and calibration of X-ray tubes.

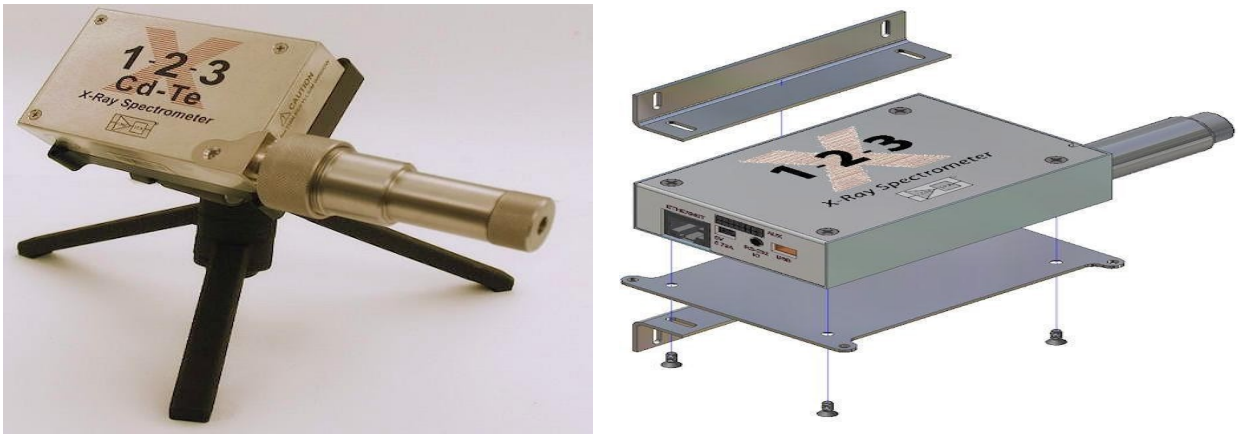

Fig. 1 CdTe Detector

From an instrumental perspective, the CdTe detector is connected to a specially designed charge-sensitive preamplifier and mounted on a thermoelectric cooling system together with the input field-effect transistor (FET). The thermoelectric cooler significantly reduces electrical noise generated within the detector and preamplifier, thereby improving measurement stability and spectral resolution. Importantly, this cooling mechanism operates automatically and remains transparent to the user, allowing the system to function similarly to a room-temperature device from the operator's perspective.

Furthermore, the charge-sensitive preamplifier incorporates a dedicated feedback mechanism that periodically injects reset pulses into the detector through the high-voltage connection. This design ensures stable signal processing and prevents signal saturation during operation. Despite the compact size of the X-123 detector system, it maintains excellent spectroscopic performance. Typically, the energy resolution measured at the 5.9 keV peak of the Fe-55 source ranges between approximately 145 eV and 260 eV full width at half maximum (FWHM), depending on the detector configuration and the selected shaping time constant.

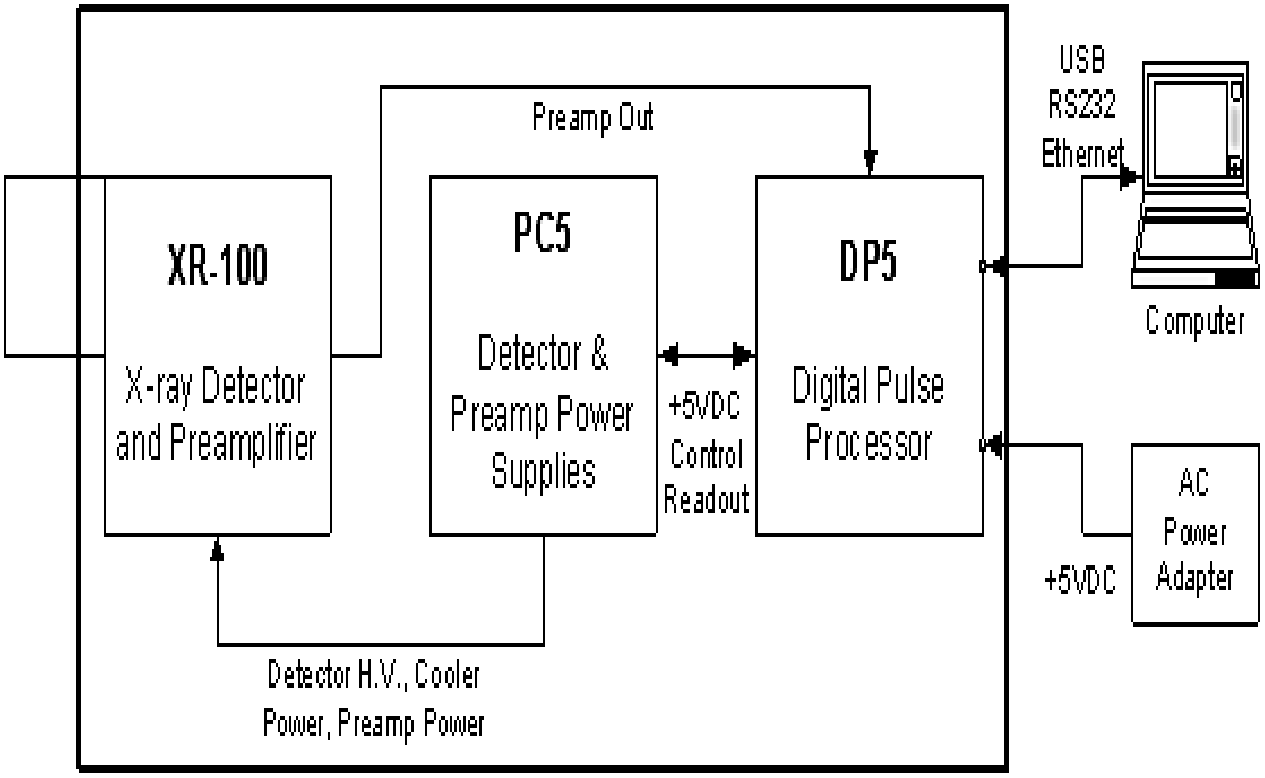

Fig. 2 X-123 Architecture and Connection Diagram

Energy Calibration Using CdTe

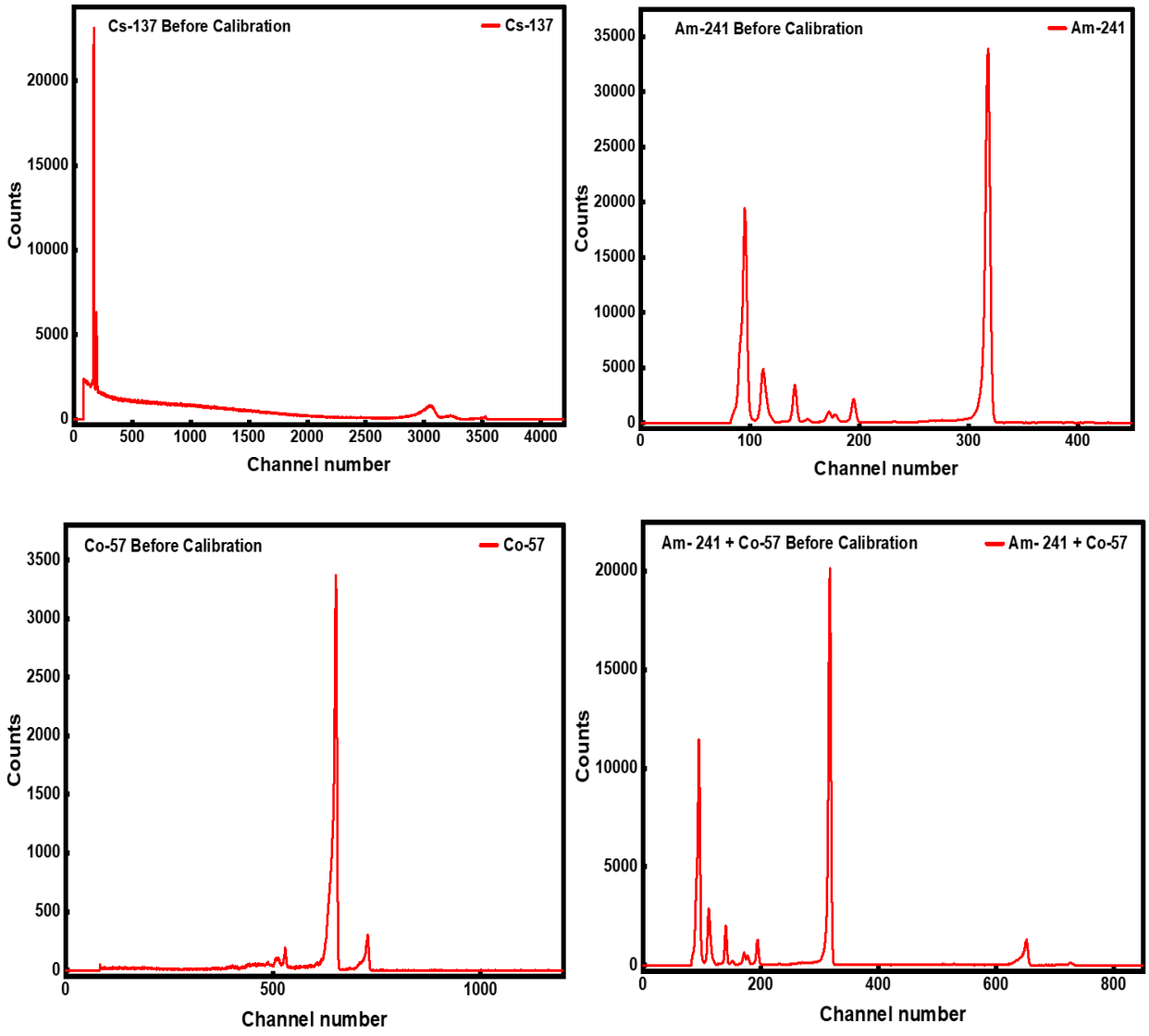

Fig.3 Energy Before Calibration by using four types of isotopes Cs-137, Am-241, Co-57 and Am-241+ Co-57 by CdTe

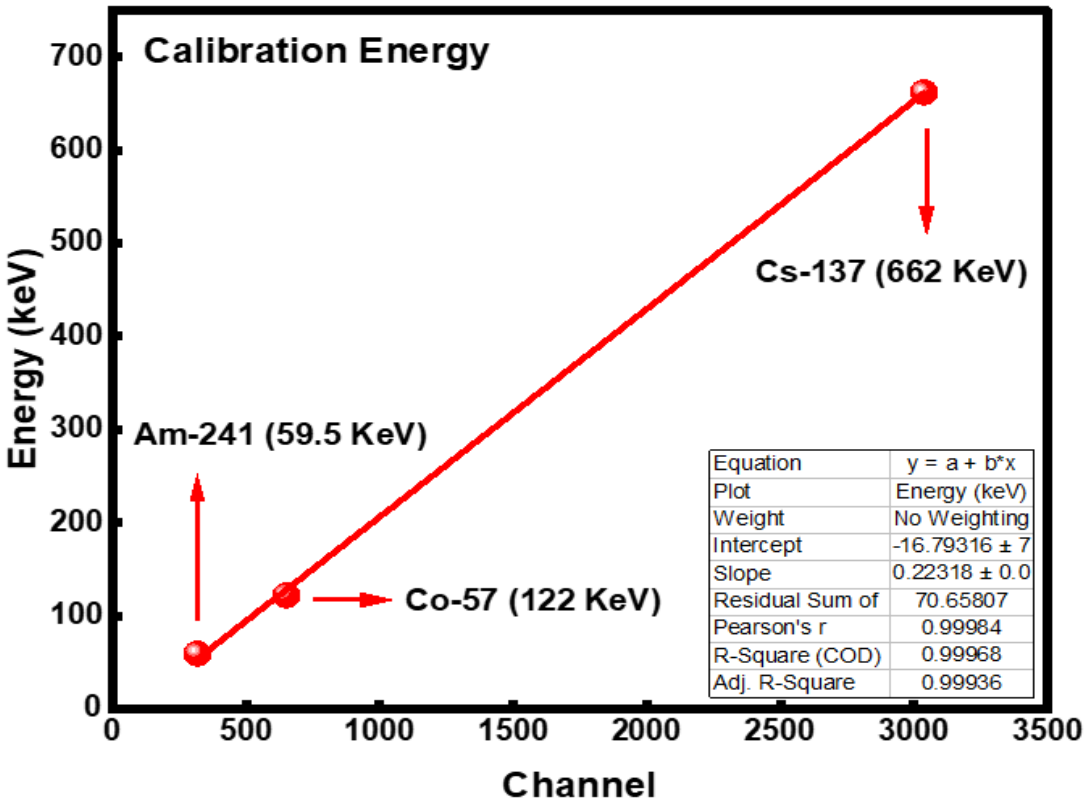

Fig.4 Energy calibration function

Source	Energy (keV)	Center (keV)	FWHM (keV)	Resolution %
Cs-137	662	661.216	21.302	3.22 %
Co-57	122	122.288	2.165	1.77 %
Am-241	59.5	58.043	1.113	1.92 %
Am-241 + Co-57	—	54.040	1.105	2.05 %
Am-241 + Co-57	—	128.271	2.142	1.67 %

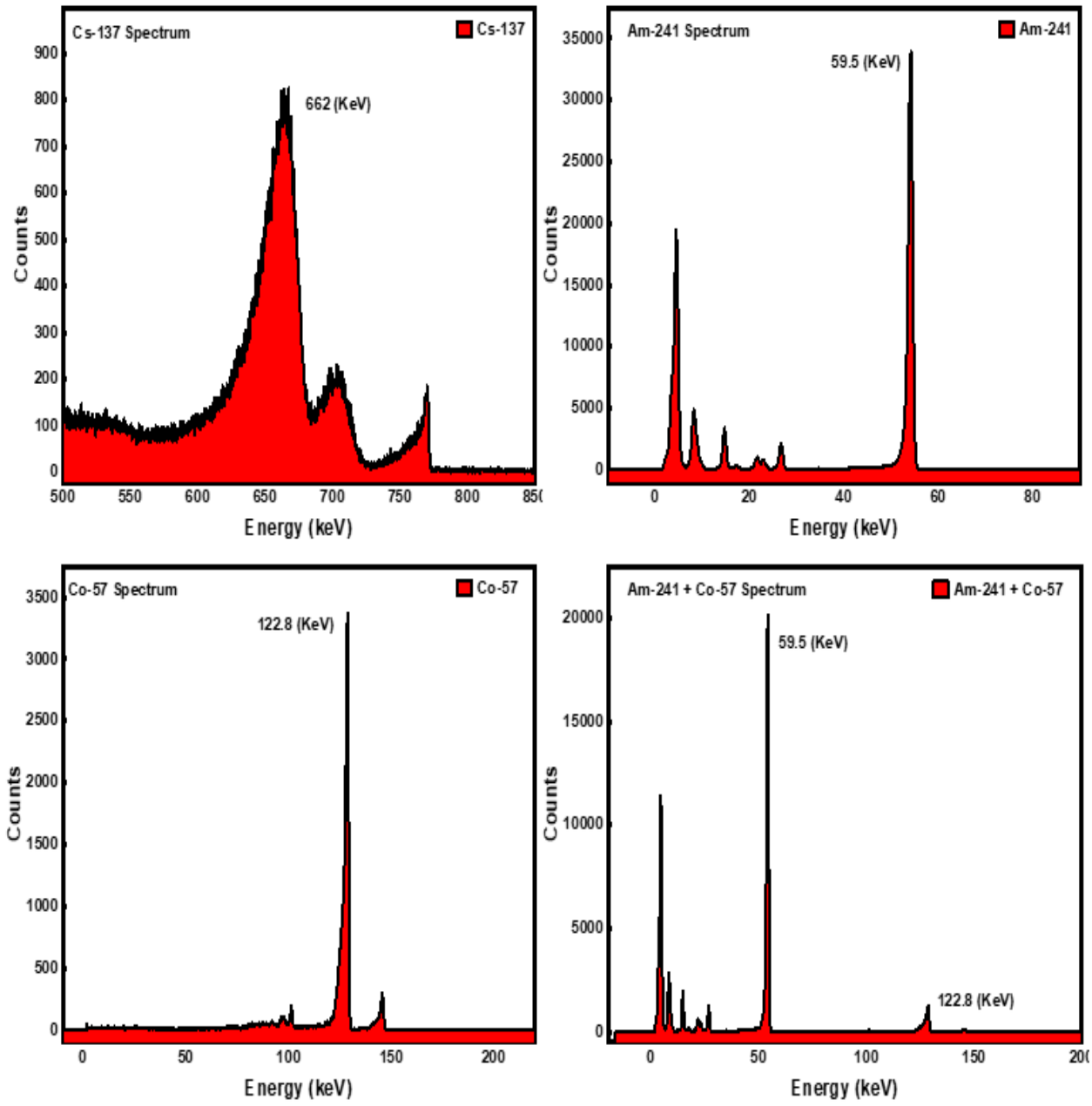

Fig.5 Calibration Energy for Am-241, Cs-137, Co-57 and Co-60

Detection Efficiency of Semiconductor Detectors

Detection efficiency is one of the most important parameters used to evaluate the performance of radiation detectors. It describes the ability of a detector to register incident radiation and convert it into a measurable signal. In semiconductor detectors, the efficiency depends mainly on the material properties, such as atomic number, density, and detector thickness, as well as the energy of the incident radiation.

Different semiconductor materials exhibit different interaction probabilities with incoming photons. Therefore, comparing the detection efficiency of various detector materials is essential in order to determine the most suitable detector for specific radiation measurements. In this study, three commonly used semiconductor materials were investigated: Cadmium Telluride (CdTe), Silicon (Si), and Gallium Arsenide (GaAs).

Efficiency Calculation Method

The detection efficiency of semiconductor detectors represents the probability that an incident photon interacts within the detector material and produces a measurable signal. This parameter is strongly influenced by the physical properties of the detector material, including the atomic number, density, detector thickness, and the energy of the incident radiation.

The detection efficiency can be estimated using the exponential attenuation law of photons in matter, which describes how radiation intensity decreases as it travels through a material.

The efficiency is calculated using the following equation:

$$\boldsymbol{\eta = 1 - e^{-\mu(E)x}}$$

Where:

η : Detection efficiency of the detector.

μ(E) : The **linear attenuation coefficient** of the material at photon energy **E** (cm^{-1}).

x: Thickness of the detector material (cm).

E: Energy of the incident photon (keV).

Linear Attenuation Coefficient

The linear attenuation coefficient μ(E) represents the probability per unit path length that a photon will interact with the detector material. It depends on both the photon energy and the atomic composition of the material.

The linear attenuation coefficient can be obtained from the mass attenuation coefficient using the relation:

$$\boldsymbol{\mu(E) = (\frac{\mu}{\rho})\rho}$$

μ/ρ: Mass attenuation coefficient (cm^2/g)

ρ: Density of the detector material (g/cm^3)

Thus, the linear attenuation coefficient depends directly on the density of the material and the photon interaction probability.

Material Density

The density of the detector material plays a crucial role in determining the interaction probability of photons with the detector. Materials with higher densities provide a larger number of atoms per unit volume, which increases the probability of photon interactions such as the **photoelectric effect**, **Compton scattering**, and **pair production**.

In this study, three semiconductor materials were investigated:

✓ Cadmium Telluride (CdTe)

CdTe is a compound semiconductor widely used for X-ray and gamma-ray detection due to its **high atomic number and relatively high density**.

$$\boldsymbol{\rho}\ \text{CdTe} = 5.85\ g/cm^3$$

The high density and large atomic numbers of cadmium (Z = 48) and tellurium (Z = 52) significantly increase the probability of photon absorption, especially through the **photoelectric interaction**. As a result, CdTe detectors exhibit very high detection efficiency even for relatively thin detector layers.

Energy (keV)	μ/ρ (cm^2/g)	Density (g/cm^3)	μ(E) (cm^{-1})	Thickness (cm)	Efficiency (%)
10	138.1	5.85	807.285	0.1	≈100
20	21.44	5.85	125.4	0.1	99.9996
30	21.82	5.85	127.587	0.1	99.9997
40	19.3	5.85	112.905	0.1	99.9987
50	10.67	5.85	62.3895	0.1	99.80
60	6.542	5.85	38.2557	0.1	97.82
70	4.321	5.85	25.2859	0.1	92.03
80	3.019	5.85	17.6532	0.1	82.87
90	2.206	5.85	12.9111	0.1	72.52
100	1.671	5.85	9.7744	0.1	62.37

CdTe detector parameters and calculated efficiency values

✓ Silicon (Si)

Silicon is one of the most commonly used semiconductor detector materials because of its excellent electronic properties and mature fabrication technology.

$$\boldsymbol{\rho}\ \mathrm{Si} = 2.33\ g/cm^3$$

However, silicon has a relatively **low atomic number (Z = 14)** and **lower density** compared with other semiconductor materials. Consequently, the probability of photon interaction within silicon is smaller, particularly at higher photon energies. This leads to a significant decrease in detection efficiency for X-rays and gamma rays.

Energy (keV)	μ/ρ (cm^2/g)	Density (g/cm^3)	μ(E) (cm^{-1})	Thickness (cm)	Efficiency (%)
10	33.88	2.33	78.9804	0.03	92.0%
20	4.463	2.33	10.4018	0.03	26.8%
30	1.436	2.33	3.3445	0.03	9.7%
40	0.701	2.33	1.6333	0.03	4.8%
50	0.4385	2.33	1.0223	0.03	3.0%
60	0.3206	2.33	0.7470	0.03	2.2%
70	0.259	2.33	0.6035	0.03	1.8%
80	0.2228	2.33	0.5191	0.03	1.5%
90	0.1996	2.33	0.4651	0.03	1.4%
100	0.1835	2.33	0.4280	0.03	1.3%

Si detector parameters and calculated efficiency values

✓ Gallium Arsenide (GaAs)

Gallium arsenide is another compound semiconductor used in radiation detection applications. It has a higher atomic number than silicon and therefore provides improved photon absorption.

$$\rho \text{ GaAs}=5.32 \text{ g/cm}^3$$

The higher density and atomic numbers of gallium (Z = 31) and arsenic (Z = 33) enhance the interaction probability compared with silicon. As a result, GaAs detectors demonstrate better efficiency than silicon detectors, particularly for medium-energy photons.

Energy (keV)	μ/ρ (cm²/g)	Density (g/cm³)	μ(E) (cm⁻¹)	Thickness (cm)	Efficiency (%)
10	37.8	5.32	201.096	0.05	99.8%
20	42.58	5.32	226.346	0.05	99.9%
30	13.97	5.32	74.3404	0.05	97.9%
40	6.262	5.32	33.3108	0.05	81.0%
50	3.365	5.32	17.900	0.05	59.6%
60	2.042	5.32	10.8574	0.05	41.2%
70	1.353	5.32	7.199	0.05	30.0%
80	0.9587	5.32	5.101	0.05	22.5%
90	0.7168	5.32	3.814	0.05	18.0%
100	0.5598	5.32	2.975	0.05	14.2%

GaAs detector parameters and calculated efficiency values

Detector Thickness

Another important parameter in the efficiency calculation is the **detector thickness**.

The probability that a photon interacts inside the detector increases with the thickness of the material because the photon travels through a larger interaction volume. In the present study, the detector thickness values used in the calculations were:

CdTe detector: x=0.1 cm Si detector: x=0.03 cm GaAs detector: x=0.05 cm

Increasing detector thickness generally improves detection efficiency, but it may also increase noise and charge collection effects in practical detector systems.

Efficiency Behavior with Photon Energy (Registration Efficiency)

Figure shows the variation of detection efficiency with photon energy for CdTe, Si, and GaAs semiconductor detectors. It can be observed that the detection efficiency decreases with increasing photon energy for all materials. This behavior occurs because the probability of photon interaction within the detector material decreases as photon energy increases.

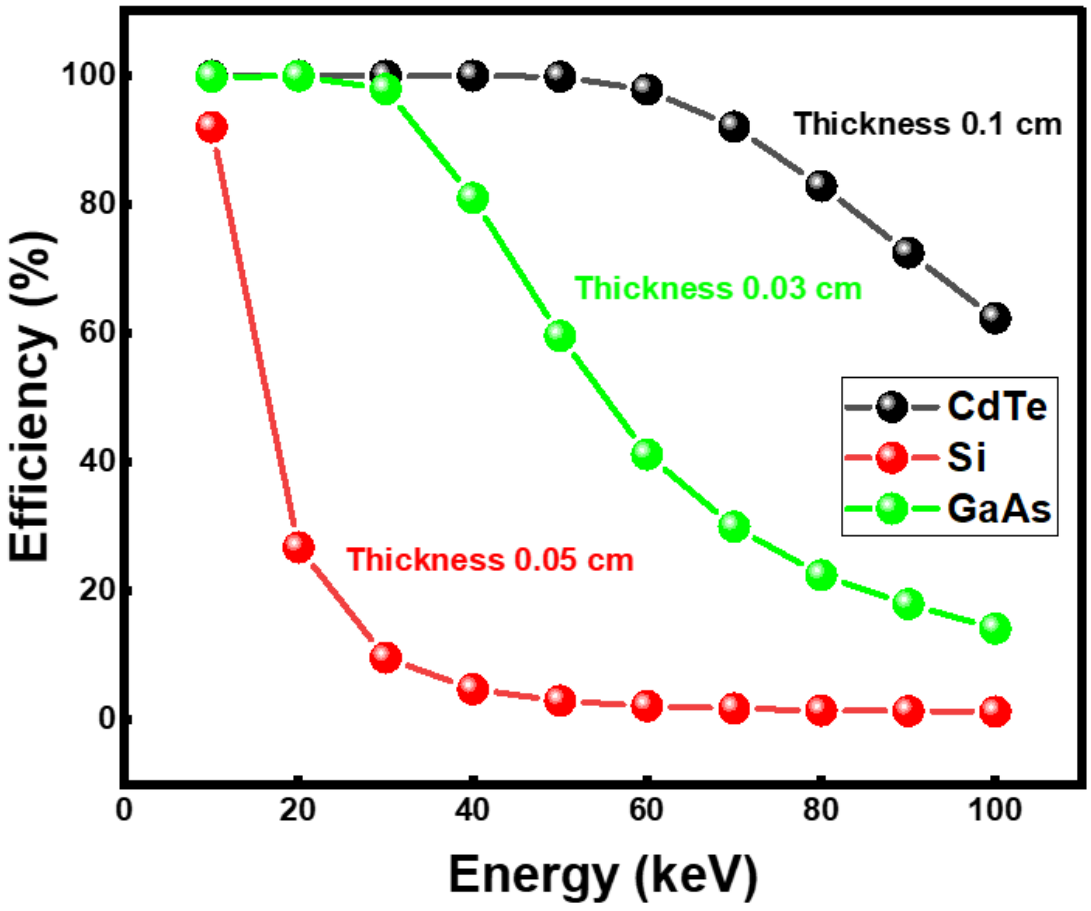

Fig.6: Detection efficiency as a function of photon energy for CdTe, Si, and GaAs semiconductor detectors.

Among the three materials, the CdTe detector exhibits the highest efficiency across the entire energy range. This is mainly due to its high density (5.85 g/cm^3) and large atomic numbers of cadmium and tellurium, which significantly increase the probability of photon absorption through the photoelectric effect.

In contrast, the silicon detector shows the lowest efficiency, particularly at higher photon energies. This is attributed to its lower density (2.33 g/cm^3) and lower atomic number, which reduce the interaction probability of photons with the detector material.

The GaAs detector demonstrates intermediate behavior between CdTe and silicon. Due to its relatively higher density (5.32 g/cm^3) and larger atomic numbers compared with silicon, GaAs provides improved efficiency but still remains lower than CdTe.

2. Scintillator detectors

Scintillation detectors are widely used in radiation measurements due to their high detection efficiency and fast response. In these detectors, the interaction of ionizing radiation with a scintillating material results in the emission of visible or ultraviolet light photons. This light is then converted into an electrical signal using a photodetector, typically a photomultiplier tube (PMT) or a photodiode. The resulting electrical pulses can be analyzed to determine important properties of the incident radiation, such as its energy and intensity.

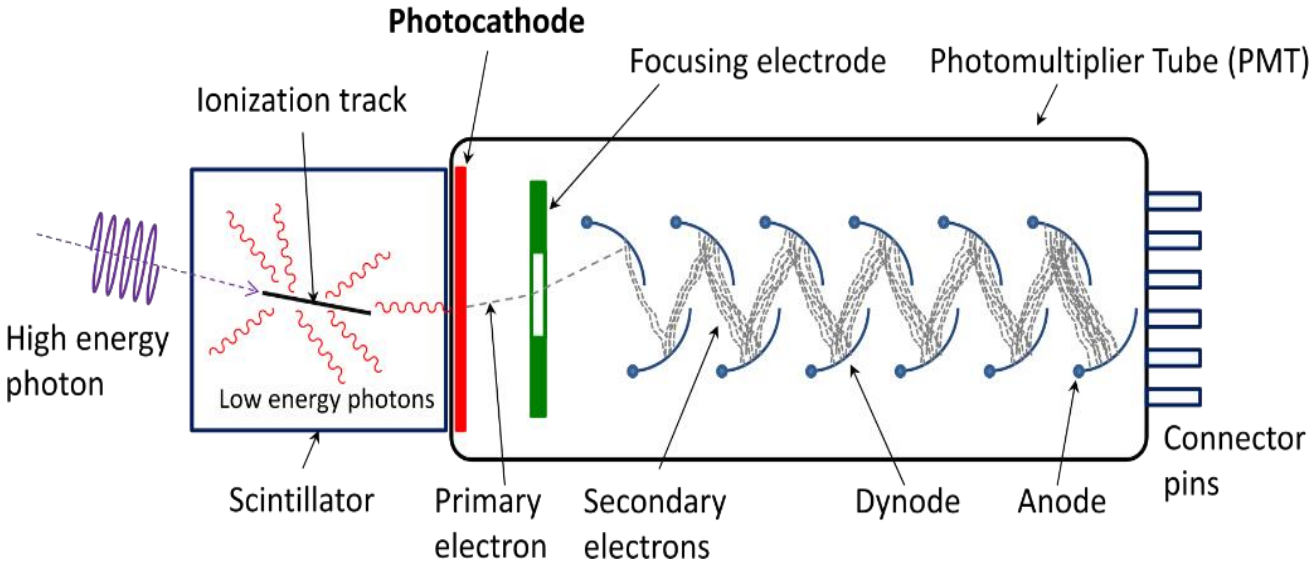

Fig.7 Scheme of scintillator detector

Scintillation materials are generally classified into two main categories:

- **Organic Scintillators:** These detectors are typically composed of organic materials such as plastics or liquid scintillators. They are particularly effective for the detection of charged particles, especially beta particles, due to their fast response time and relatively low density.
- **Inorganic Scintillators:** These detectors are commonly made from crystalline materials and are widely used for gamma-ray detection. One of the most common examples is sodium iodide (NaI), which provides high light output and good detection efficiency for gamma radiation.

In addition to NaI, several advanced inorganic scintillation materials have been developed to improve radiation detection performance. Materials such as bismuth germanate (BGO) and lanthanum bromide ($LaBr_3$) are widely used in modern radiation detection systems because of their high density and excellent gamma-ray stopping power. These properties make scintillation detectors particularly useful in nuclear spectroscopy, environmental monitoring, and medical imaging applications.

LaBr Scintillator Detector

The $LaBr_3$ (Lanthanum Bromide) detector utilizes a lanthanum bromide crystal as its scintillation medium, offering a highly efficient platform for gamma-ray spectroscopy. These detectors are renowned for their rapid response times and exceptional energy resolution, making them particularly advantageous over conventional scintillators such as sodium iodide (NaI). The superior resolution of $LaBr_3$ enables precise identification and accurate quantification of gamma-ray energies, which is critical in nuclear physics experiments, environmental monitoring, and medical imaging applications.

$LaBr_3$ crystals exhibit a remarkably short scintillation decay time, typically around 16 nanoseconds, allowing the detector to operate effectively at high count rates while minimizing the occurrence of pulse pile-up. Additionally, their high light yield produces strong, well-defined signals, improving the signal-to-noise ratio and enhancing overall detector performance. Intrinsically, $LaBr_3$ detectors achieve a resolution of approximately 2.5% at 662 keV (from a Cs-137 source), significantly outperforming the 6–7% resolution commonly observed in NaI(Tl) detectors.

The combination of rapid decay, high efficiency, and excellent resolution extends the applicability of $LaBr_3$ detectors to complex spectral analyses and demanding experimental conditions that were previously challenging for standard scintillation detectors. This makes $LaBr_3$ an indispensable tool in fields requiring high precision, reliability, and speed, from fundamental research to advanced radiation detection systems.

Calculation of resolution of LaBr3 at different applied voltages

$LaBr_3$ detectors exhibit a relatively strong intrinsic background due to the decay of ^{138}La, which limits their suitability for low-level radiation measurements. The resolution of a $LaBr_3$ detector quantifies its ability to accurately determine the energy of incident radiation and to differentiate it from adjacent energy peaks. This resolution is calculated as the ratio of the full width at half maximum (FWHM) of a spectral peak to its centroid position, expressed mathematically as:

$$\text{Resolution } (\%) = \frac{FWHM}{Centroid} \times 100 = \frac{\sigma \times 2.35}{Mean} \times 100$$

Here, σ represents the standard deviation of the peak, and the factor 2.35 converts it to FWHM.

Energy resolution is a critical parameter in gamma-ray spectroscopy, as it determines the detector's capability to resolve closely spaced energy peaks. A lower energy resolution value corresponds to enhanced discrimination between neighboring peaks, facilitating the precise identification of individual radionuclides and decay processes within complex radiation spectra. This characteristic is particularly important when analyzing spectra with overlapping peaks or in high-precision nuclear measurements.

Table:

Applied Voltage (V)	Mean	Sigma	Resolution (%)
700	1.663	0.089	12.58
700	1.903	0.068	8.40
750	3.076	0.1418	10.84
750	3.504	0.1181	7.92
800	5.2333	0.2435	10.93
800	5.9686	0.1964	7.73
900	13.7411	0.6168	10.55
900	15.5638	0.4924	7.44

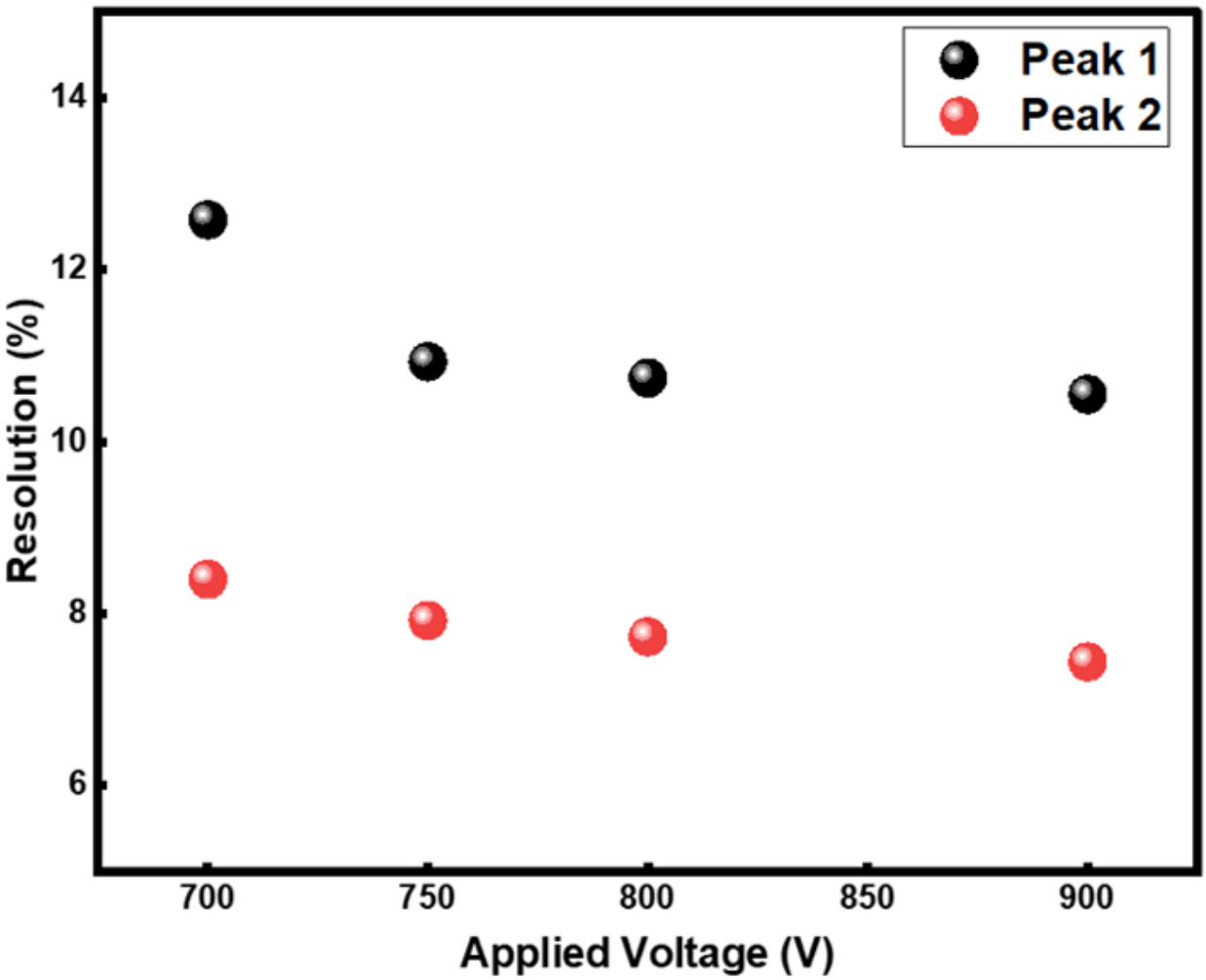

Fig.8 The relation between resolution and applied voltage for $LaBr_3$ detector.

In applications demanding high-resolution detection of Co-60 gamma emissions, the energy resolution of $LaBr_3$ detectors improves markedly with increasing applied voltage. This enhancement is primarily attributed to an increased signal-to-noise ratio at higher voltages, which enables more precise discrimination of gamma-ray energies. Consequently, careful optimization of the applied voltage is essential to achieve the detector's maximum performance in gamma spectroscopy.

These observations highlight the critical importance of fine-tuning detector operating parameters to enhance both the accuracy and reliability of radiation measurements. Such optimization is vital not only for fundamental research in nuclear and radiation physics but also for practical applications in medical imaging, environmental monitoring, and nuclear safety assessments.

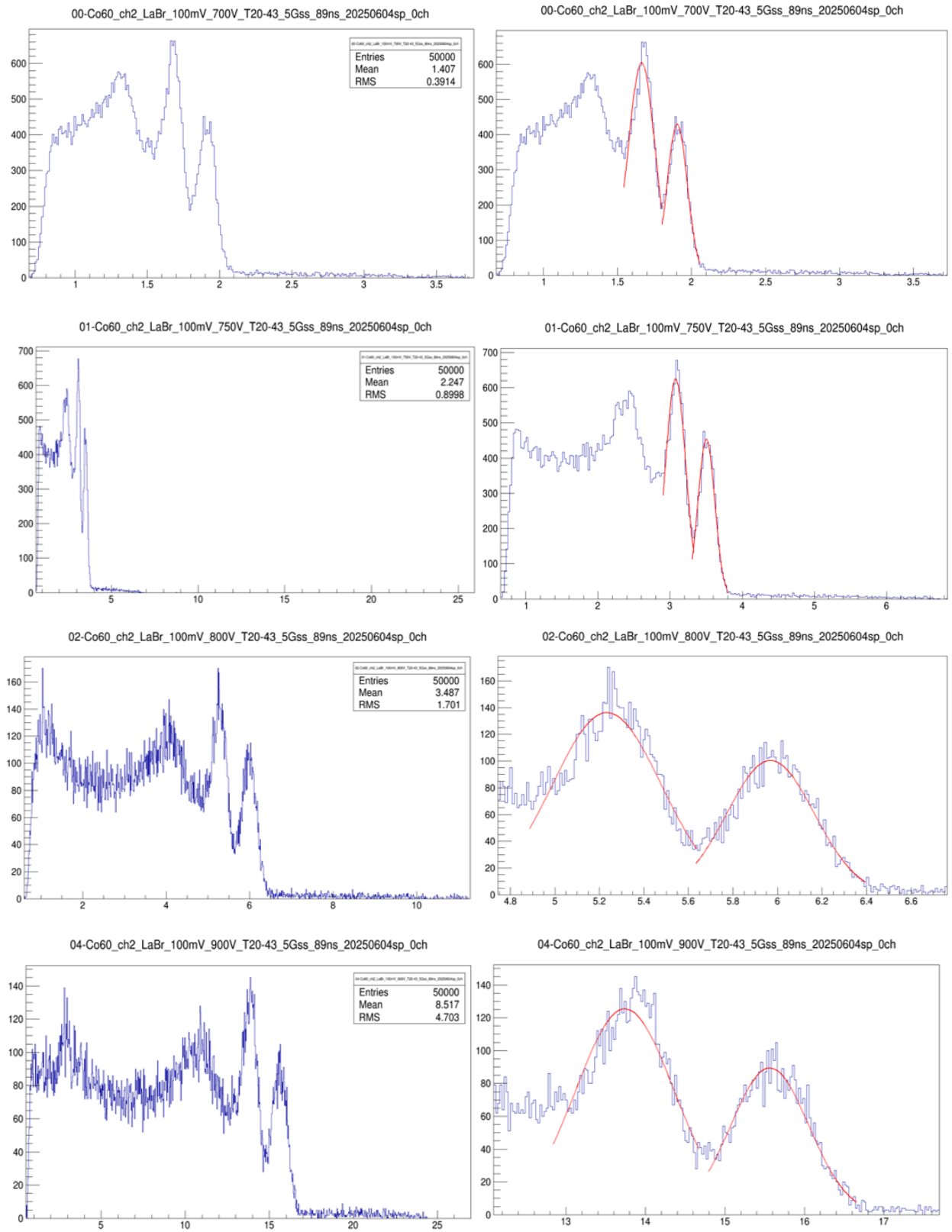

Fig.9 spectrum of Co-60 using $LaBr_3$ detector at 700,750,800,900 applied voltages

Calibration energy using LaBr3 detector

To establish the relationship between the energy and the corresponding channel number (mean), known gamma sources such as Co-60 and Cs-137 are employed. The first peak observed in the spectrum does not correspond to the energy of either source; rather, it arises from electronic noise associated with the detector's resolution. The first genuine energy peak, corresponding to Cs-137, appears at the leftmost position of the spectrum. In contrast, Co-60 exhibits three distinct energy peaks.

Gaussian fitting is applied to these peaks using the ROOT software in order to determine the channel number (mean) for each energy. Subsequently, a calibration curve is generated by plotting energy against channel number, and the resulting linear equation provides a quantitative relation between the detector's channel output and the corresponding gamma-ray energy. This calibration process is essential for accurate spectral analysis and precise determination of unknown radiation energies.

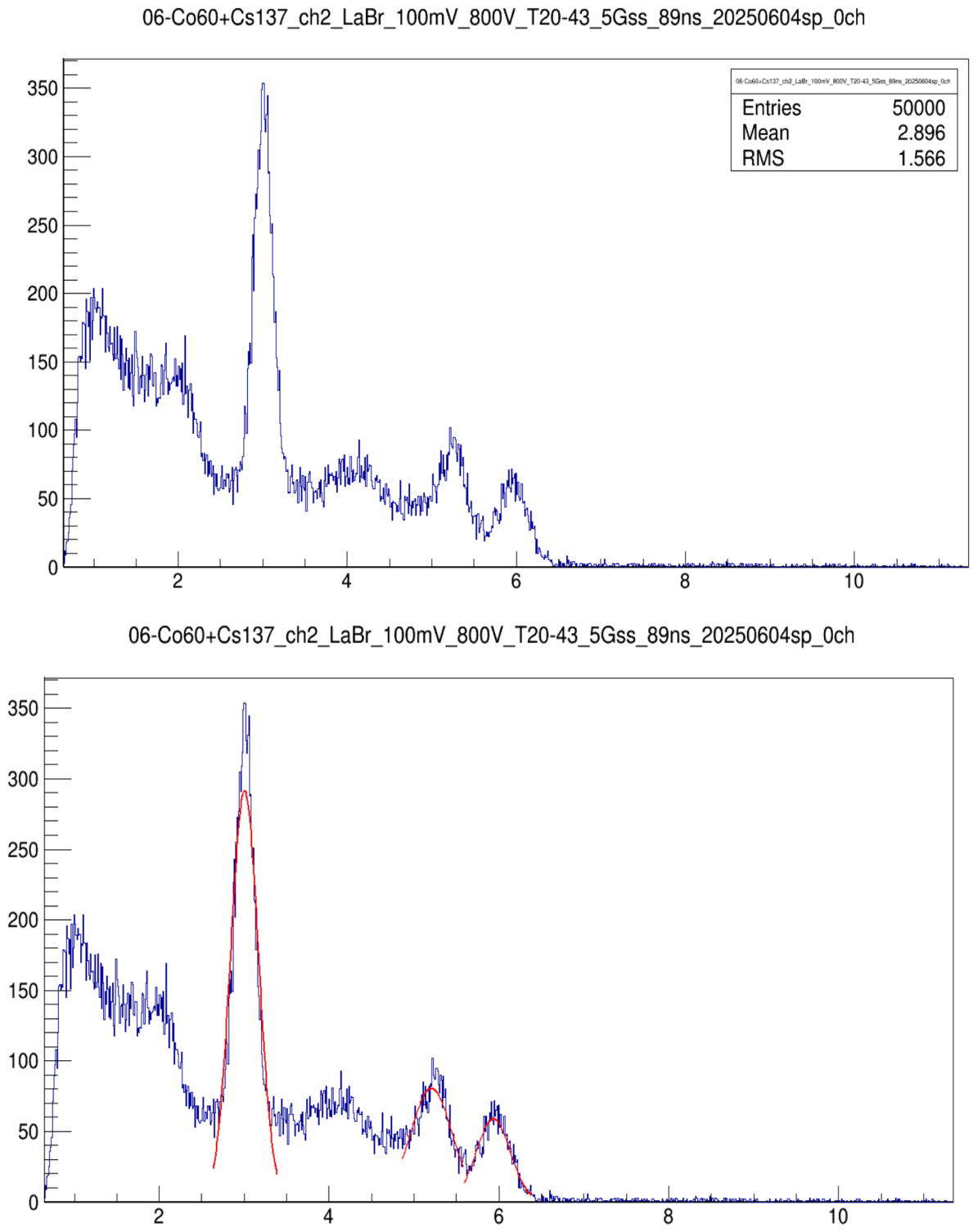

Fig. 10 The energy spectrum of Cs-137 and Co-60 from LaBr3 detector measurements at 800V.

Element	Energy (KeV)	Channel Number (Mean)	Sigma
Cs-137	662	3.00509	0.1642
Co-60	1180	5.2043	0.2455
	1330	5.9336	0.2005

Table: Mean and energy of Cs-137 and Co-60 peaks from $LaBr_3$ detector

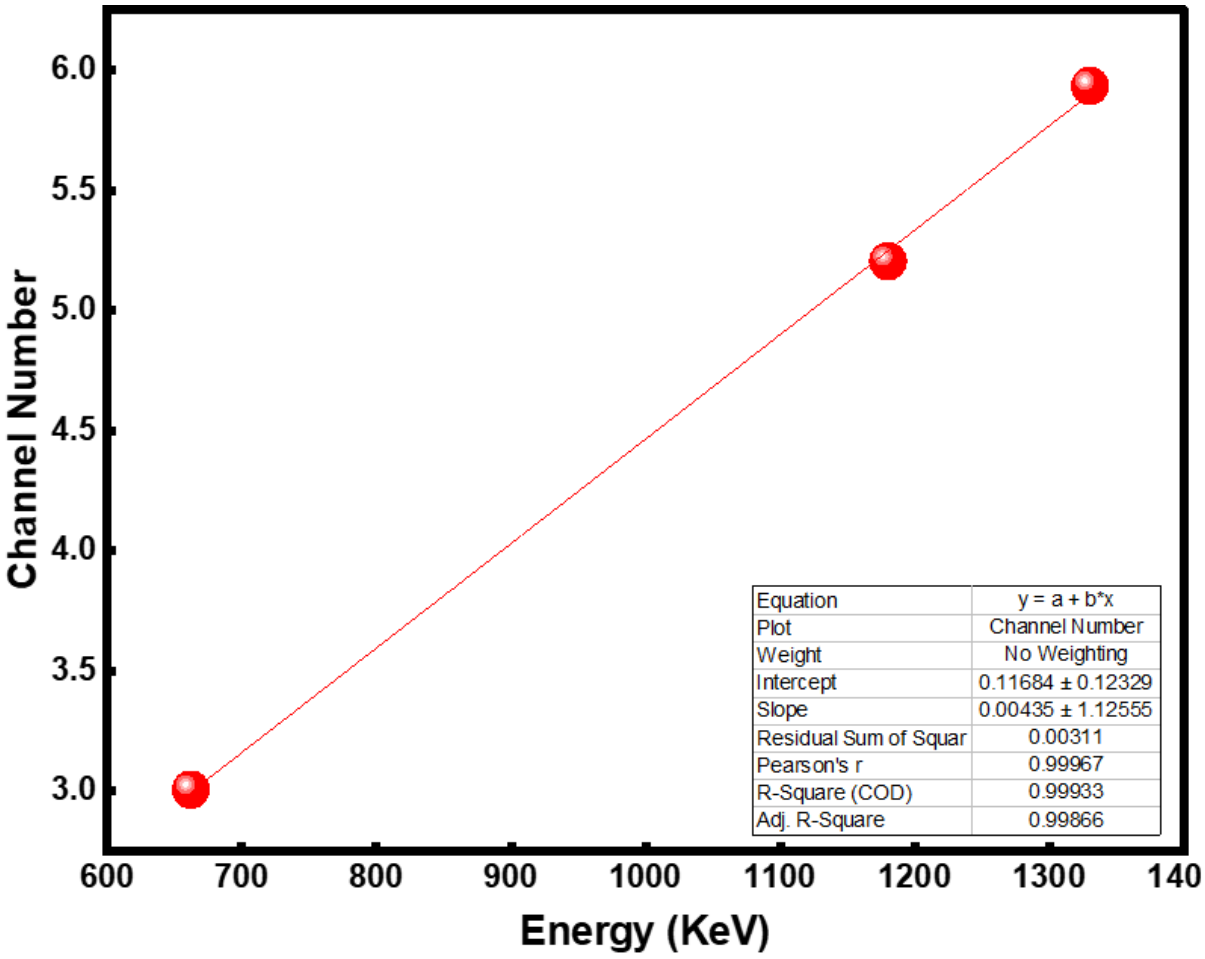

Fig. 11 Energy calibration function for Cs-137 and Co-60 spectrum from $LaBr_3$ detector measurements.

Bismuth Germinate (BGO) Detector

The BGO (Bismuth Germinate, $Bi_4Ge_3O_{12}$) detector is a type of scintillation detector that utilizes a high-density, high atomic number (Z) scintillating material. Its high gamma-ray absorption efficiency makes it particularly suitable for detecting high-energy radiation such as X-rays and gamma rays. Additionally, BGO is non-hygroscopic and mechanically robust, ensuring stable and durable operation under various experimental conditions.

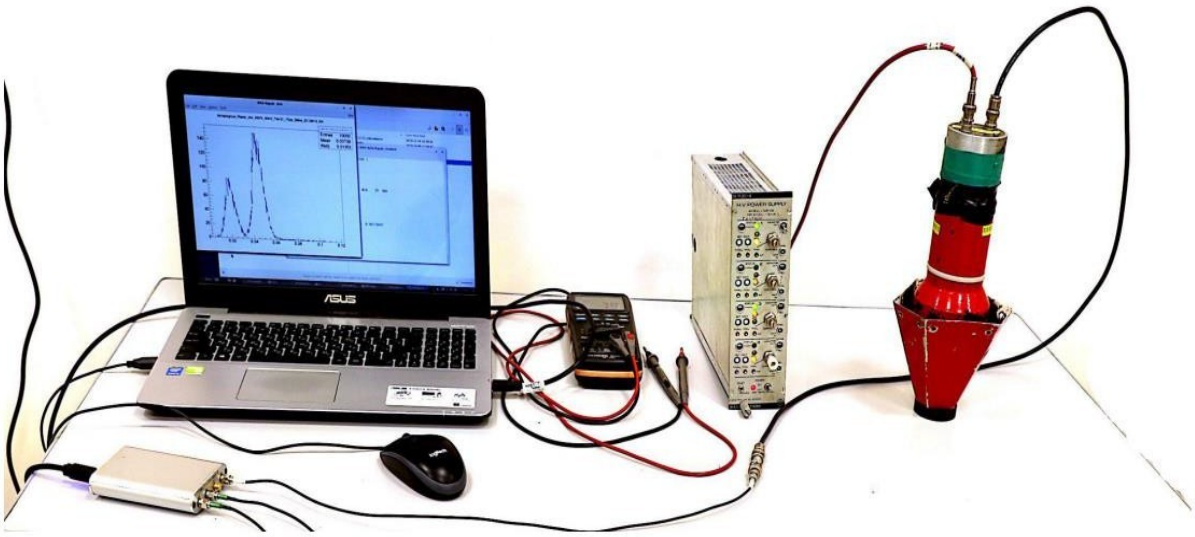

Fig. 12 BGO detector

Due to its large effective atomic number, BGO minimizes inter-crystal scatter and enhances detection efficiency. As a result, BGO detectors are widely employed in positron emission tomography (PET), radiation detection, medical imaging, radiopharmaceutical studies, security surveillance, and geological surveying.

For energy resolution analysis, Gaussian fitting is applied to the detector's spectral peaks at various applied voltages to determine the mean (centroid) and standard deviation (σ) of each peak. The resolution is then calculated using the equation:

$$\text{Resolution } (\%) = \frac{FWHM}{Centroid} \times 100 = \frac{\sigma \times 2.35}{Mean} \times 100$$

Here, σ represents the standard deviation of the peak, and the factor 2.35 converts it to FWHM.

This process allows for precise evaluation of the detector's capability to discriminate between closely spaced energy peaks under different operating conditions.

Applied Voltage (V)	Mean	Sigma	Resolution (%)
1200	1.39	0.618	104.4
1300	1.37	0.268	44.59
1400	1.92	0.291	35.49
1500	2.98	0.459	35.48
1600	4.40	0.576	30.76
1700	6.10	0.774	29.81
1900	10.6	1.292	28.6
2000	13.60	1.562	26.95

Table: Resolution (%) of BGO detector corresponding to the applied voltage

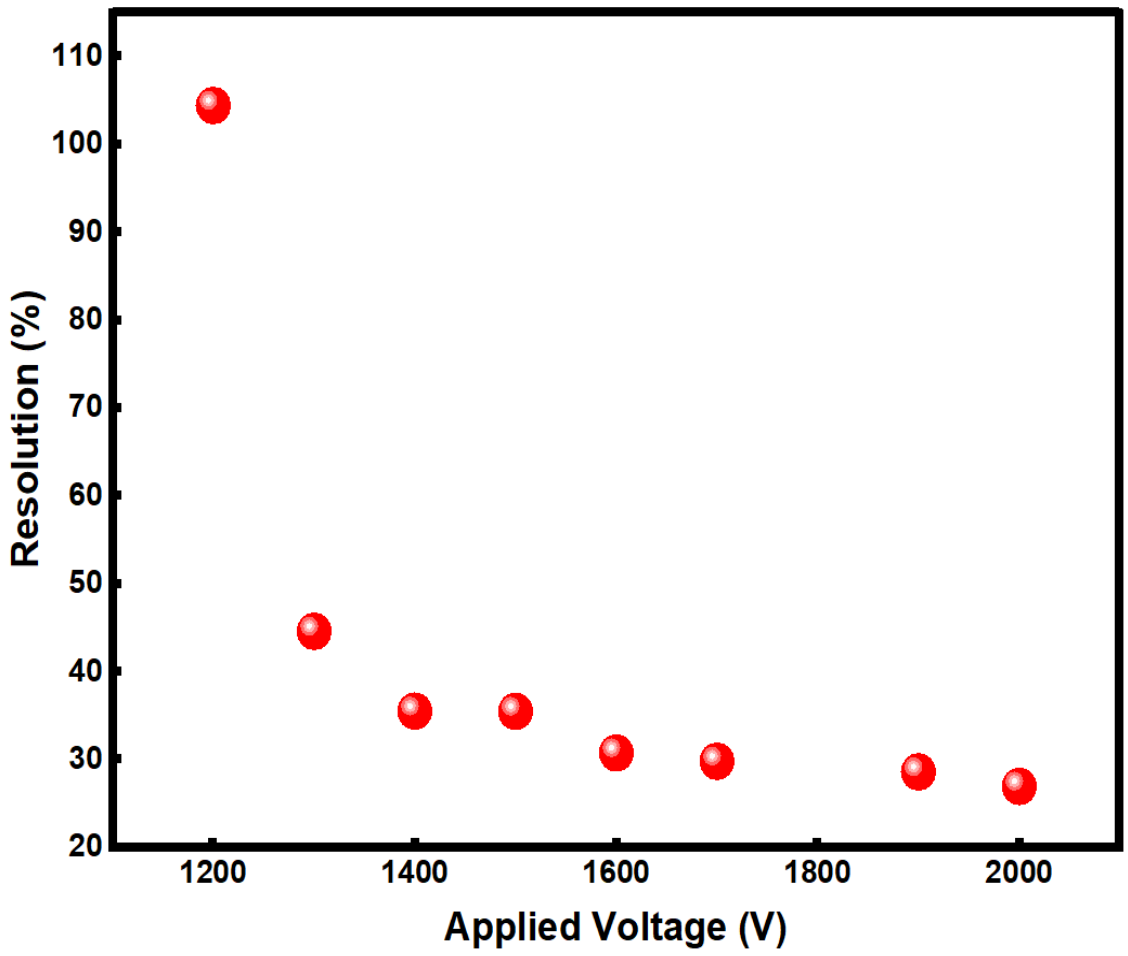

Fig. 13 The relation between resolution and applied voltage for BGO detector

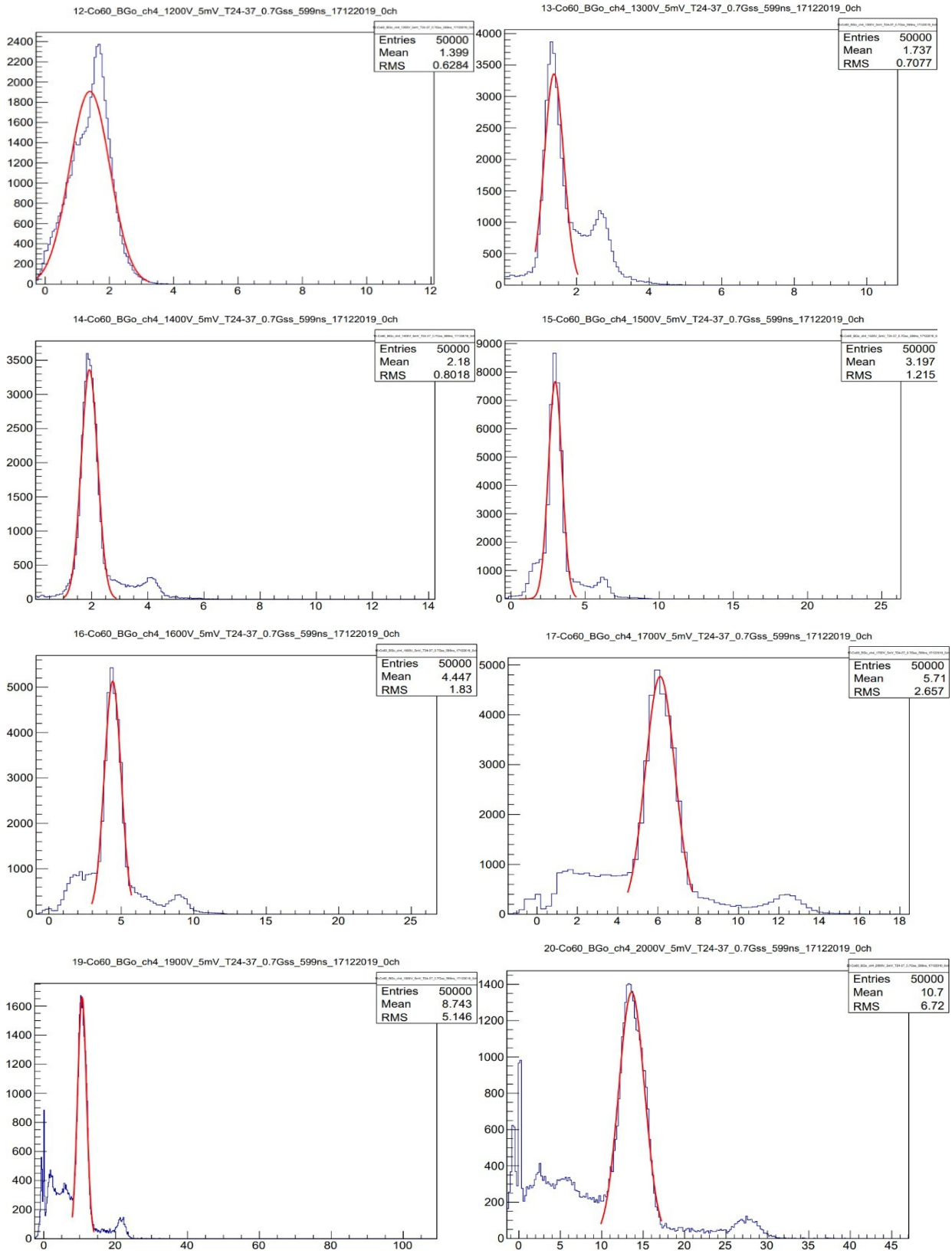

Fig. 14 spectrum of Co-60 using BGO detector at applied voltages from range 1200 to 2000V.

Calibration energy using BGO detector

Energy calibration establishes the relationship between the channel number (mean) and its corresponding gamma-ray energy. To achieve this, sources with known energy peaks, such as Co-60 and Cs-137, are employed. The first peak observed in the spectrum does not correspond to the energy of either source; it arises from electronic noise due to the detector's resolution. The first genuine energy peak, corresponding to Cs-137, appears at the leftmost position of the spectrum, whereas Co-60 exhibits two distinct energy peaks.

Gaussian fitting is performed on these peaks using the ROOT software to determine the channel number (mean) for each energy. Subsequently, a calibration curve is constructed by plotting energy against channel number, and the resulting linear equation provides a quantitative relationship between the detector's channel output and the actual gamma-ray energy. This calibration is essential for accurate spectral analysis and precise measurement of unknown radiation energies using the BGO detector.

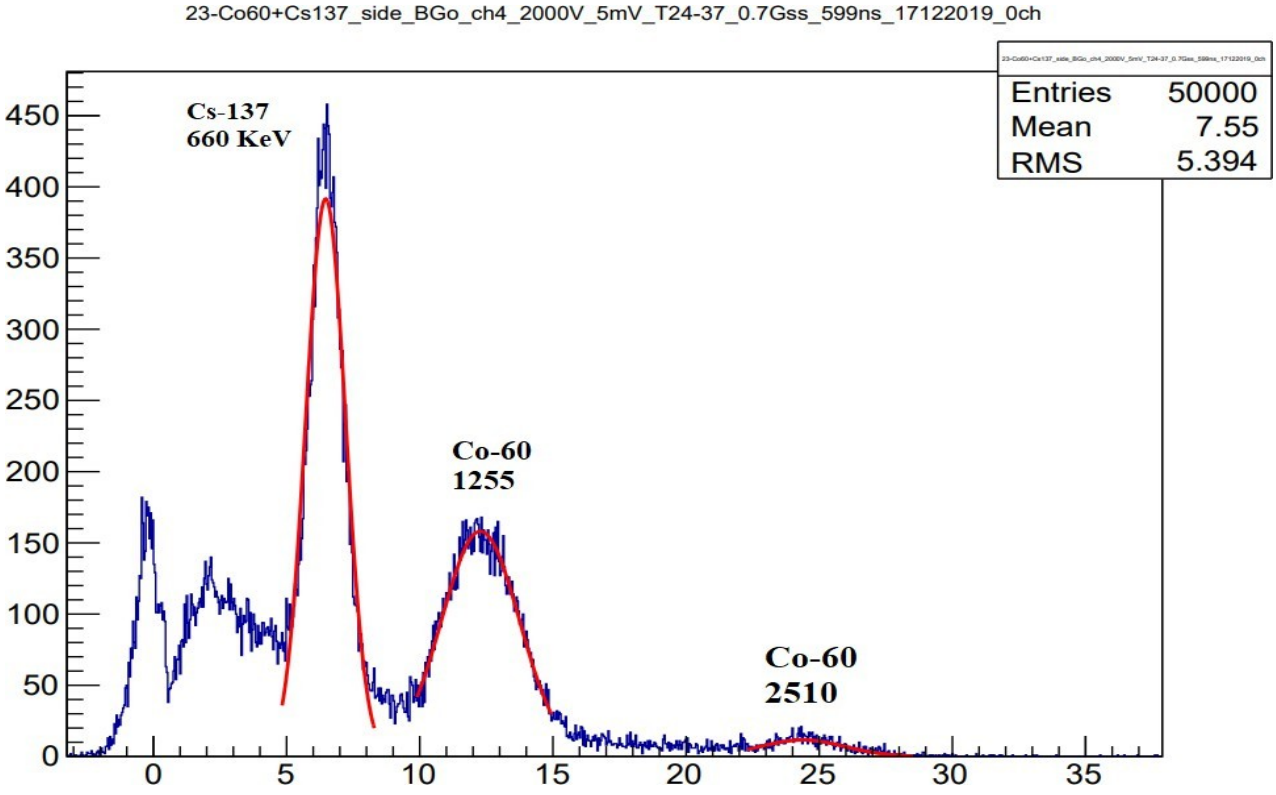

Fig. 15 The energy spectrum of Cs-137 and Co-60 from BGO detector measurements at 2000V.

Calibration equation is

$$y = 9.7284x + 0.0458$$

Element	Energy (KeV)	Channel Number
Cs-137	660	6.47
Co-60	1255	12.27
Co-60	2510	24.57

Table: Mean and energy of Cs-137 and Co-60 peaks from a BGO detector.

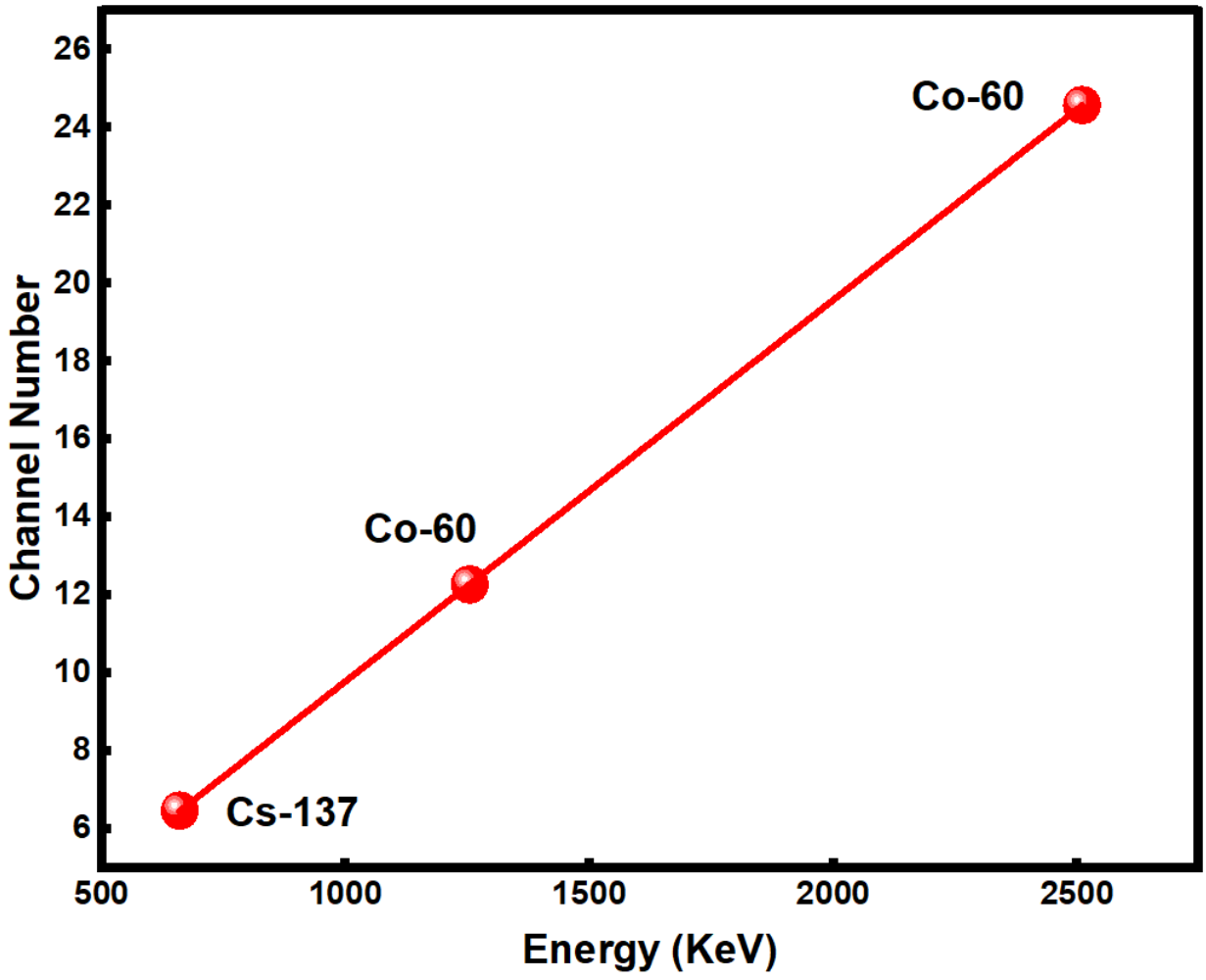

Fig.16 Energy calibration function for Cs-137 and Co-60 spectrum from BGO detector measurements.

Pixel Detector Structure and Technology

A pixel detector is an advanced detection device consisting of two integral components: the sensor chip and the readout electronics chip. The sensor chip is typically a semiconductor diode that incorporates a pixelated front contact and a common backside, which is coated with a thin layer of nickel. This nickel coating not only provides uniform electrical grounding but also enhances the mechanical robustness and stability of the detector under varying operational conditions. Each pixel functions as an independent detection unit, allowing for precise spatial localization of incident particles or photons.

The readout electronics chip is intimately coupled to the sensor chip and provides dedicated electronic channels for each individual pixel. These channels perform amplification, shaping, digitization, and transmission of the detected signals. To achieve a reliable and precise connection between the sensor and the electronics chip, the bump-bonding technique is employed. This method involves microscopic metallic contacts that enable robust mechanical and electrical integration while maintaining minimal signal loss and crosstalk between adjacent pixels.

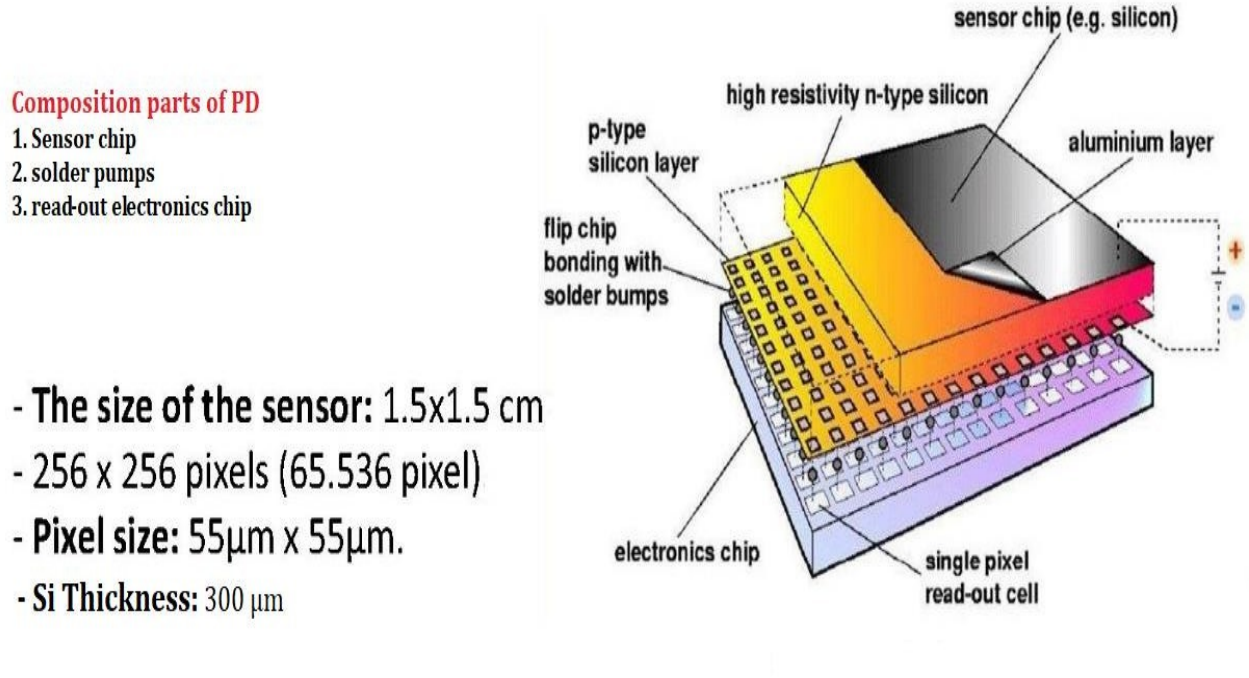

Fig. 17 Pixel detector

Pixel dimensions typically range from 100 to 400 μm, enabling high spatial granularity and excellent resolution. This fine segmentation is particularly critical in high-precision applications, including X-ray imaging, particle tracking in high-energy physics experiments, synchrotron radiation studies, and advanced medical imaging techniques. The modularity of pixel detectors also allows for scalable designs, facilitating large-area coverage without compromising resolution. Moreover, the combination of independent pixel operation, high granularity, and efficient readout electronics contributes to superior signal-to-noise performance, rapid data acquisition, and the capability to resolve complex spatial and temporal event patterns.

Determination alpha particles range with (Am-241) in Air at diffrent energy (MeV) Using pixel detector

Positively charged particles known as alpha particles are released spontaneously from the nuclei of some radioactive materials. With an electrostatic charge of +2, it is a helium ion. The components of alpha particles are two protons and two neutrons bonded together. Range is the distance that alpha particles travel before losing all their kinetic energy and recombining with electrons to produce stable helium atoms.

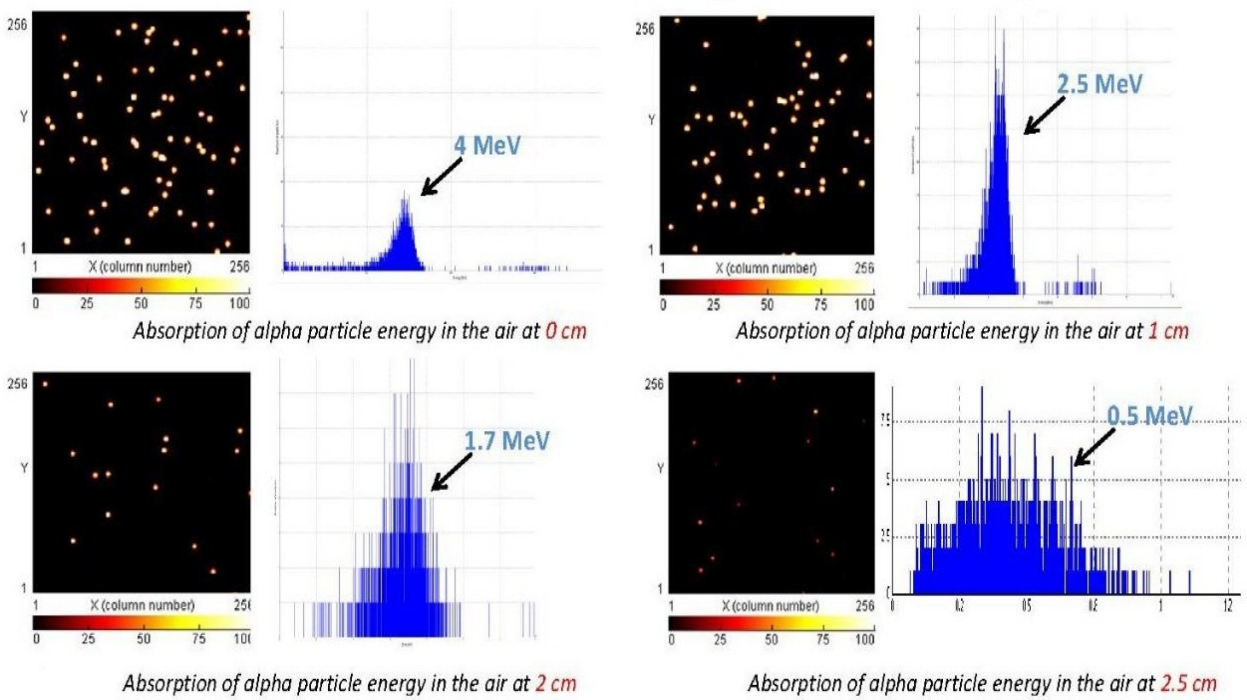

Fig. 18 Absorption of alpha particle energy in air at different thicknesses

Determination of alpha range in air using SRIM (Monte Carlo simulation)

SRIM (Stopping and Range of Ions in Matter) is a widely used simulation software that allows researchers to model and analyze ion interactions within solid materials. It provides detailed predictions of phenomena such as ion penetration depth, energy deposition, and particle range, making it an essential tool in radiation physics and materials science. Alpha particles, due to their relatively large mass thousands of times greater than that of atomic electrons interact primarily through ionization, causing a gradual energy loss while traveling in nearly straight trajectories. This characteristic makes their range in matter relatively predictable compared to lighter particles such as electrons.

In this experiment, a pixel detector is employed to measure the range of alpha particles in air. The measurement is performed by systematically varying the distance between the alpha source and the detector until the detector no longer registers any alpha events. This maximum measurable distance corresponds to the alpha particle's range, which, in our setup, is approximately 3 cm. Such measurements provide valuable experimental verification of theoretical predictions obtained from SRIM simulations and help in understanding the energy loss mechanisms and range characteristics of alpha radiation in gaseous media.

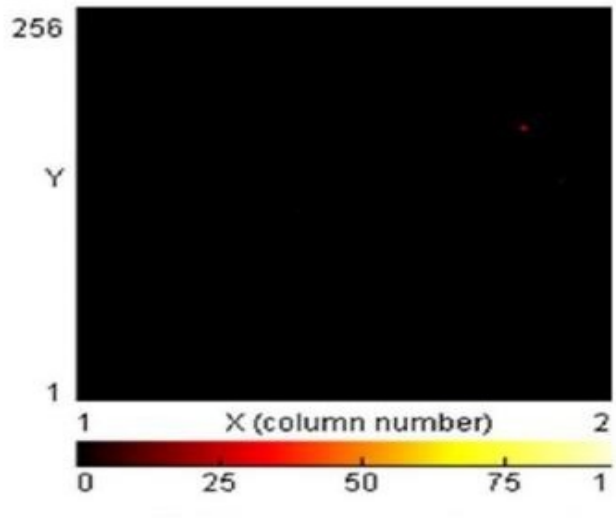

Fig. 19 Maximum of alpha particles range

Determination the range of alpha particles with Am-241 energy about 4 MeV in air using pixel detector. There is no alpha particles at 3 cm distance and maximum of alpha particle range is 3 cm.

Determining the range of alpha particles experimentally can be challenging. Therefore, SRIM software is utilized to perform Monte Carlo simulations of alpha particle interactions with various materials, including air, as illustrated in the figure below.

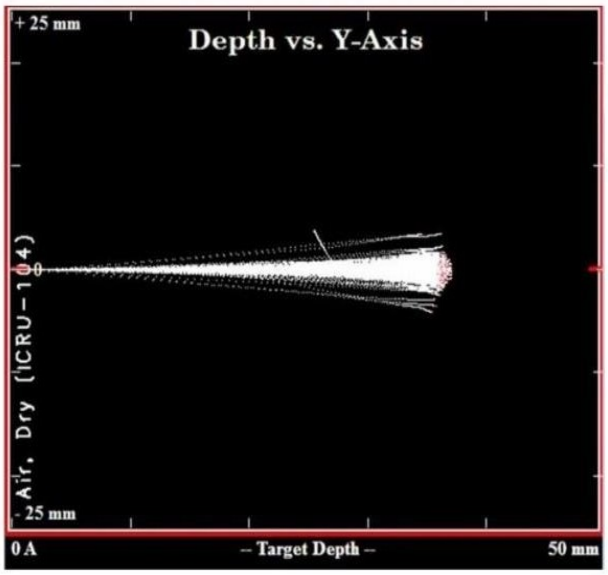

Fig. 20 Depth for alpha radiation in air

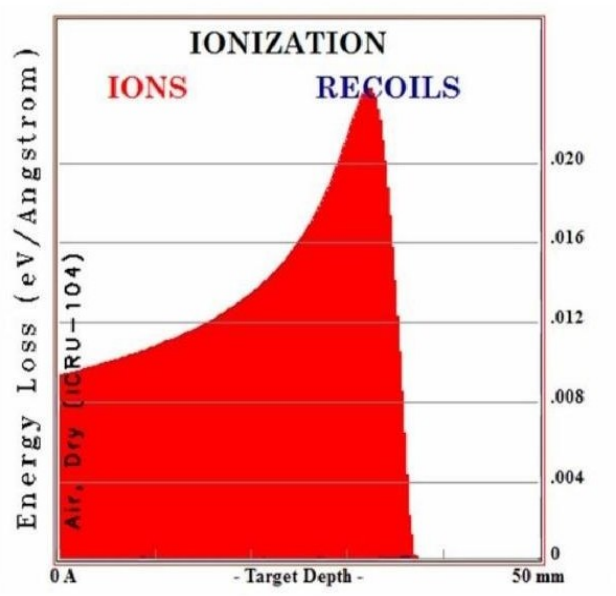

Fig. 21 Ionization – Depth graph for alpha

SRIM (Stopping and Range of Ions in Matter) is a specialized software program designed to calculate the stopping power and penetration range of ions as they traverse various materials. It is widely applied in fields such as ion implantation, radiation damage studies, and materials science research. The software employs the Monte Carlo simulation technique to model ion-matter interactions with high precision.

SRIM provides critical information on ion behavior, including penetration depth, energy deposition, and sputtering rates, which are essential for understanding both fundamental and applied aspects of ion interactions. In the present study, alpha particles with an energy of 1500 keV were simulated, producing results that serve as a benchmark for comparison with experimental measurements of alpha particle range in air and other media.

Measurement of Alpha Particle Range in Air Using a GaAs Pixel Detector

Alpha Particles

Alpha particles are heavy charged particles consisting of two protons and two neutrons. They are emitted during the radioactive decay of heavy nuclei such as radium and radon. Due to their relatively large mass and double positive charge, alpha particles interact strongly with matter, losing energy rapidly through ionization and excitation processes. As a result, their penetration depth in air is very limited, typically a few centimeters depending on their initial energy.

In this experiment, the range of alpha particles in air was measured using a GaAs pixel detector and a Ra-226 alpha source. The detector was placed at different distances from the source, and the number of detected counts per second was recorded at each position. As the distance between the source and the detector increases, alpha particles gradually lose energy through interactions with air molecules, leading to a decrease in the detected count rate. The measurements were continued until the detected counts dropped to zero, indicating that the alpha particles could no longer reach the detector.

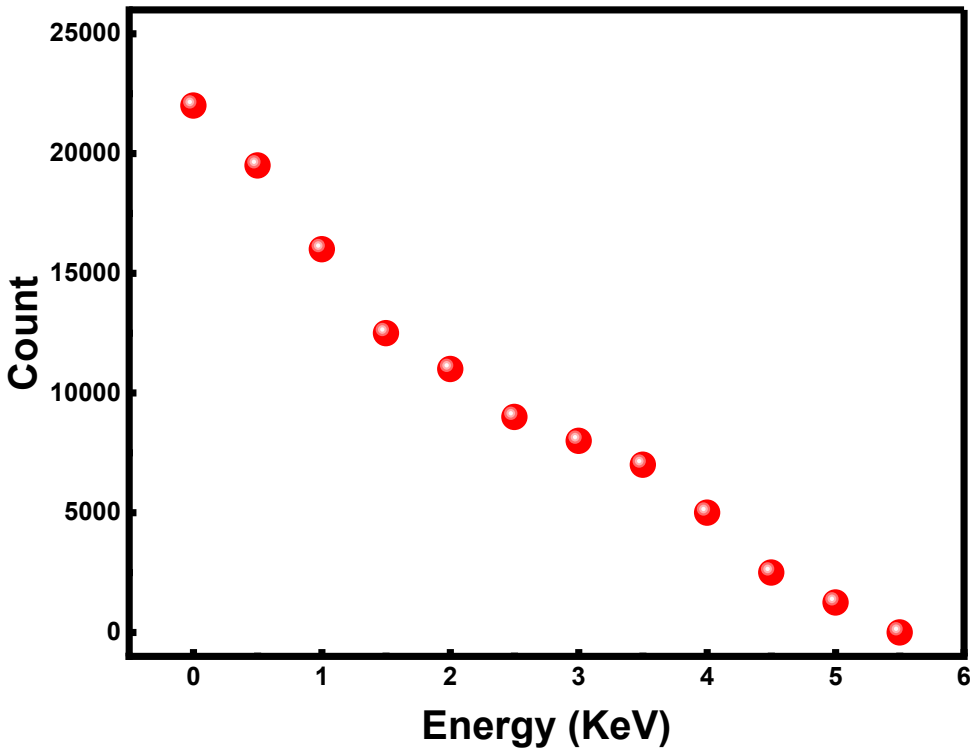

Fig.22: Variation of alpha particle counts with distance between the Ra-226 source and the GaAs pixel detector in air.

Alpha Particle Range Behavior:

Figure X shows the variation of detected alpha particle counts as a function of the distance between the Ra-226 source and the GaAs pixel detector. The results clearly demonstrate a gradual decrease in the detected count rate as the distance increases. This behavior occurs because alpha particles lose energy through ionization and excitation processes while traveling through air.

As the alpha particles propagate through the air, they continuously interact with air molecules, which reduces their kinetic energy. Eventually, the particles lose all their energy and stop completely, resulting in zero detected counts. In this experiment, the count rate reaches zero at a distance of approximately 5.5 cm, which corresponds to the maximum range of the alpha particles in air under the given experimental conditions. The measured stopping distance represents the **practical range** of alpha particles in air.

X-ray Spectrum Analysis Using CdTe Detector

Simulation Results

To investigate the intrinsic response of the CdTe detector, X-ray spectra were simulated at incident energies of 20, 40, 60, 80, and 100 keV. These simulations provide an ideal representation of the detector behavior under controlled conditions, excluding most real-world imperfections.

The simulated spectra exhibit smooth distributions with well-defined shapes that evolve systematically with increasing photon energy. As the incident energy increases, both the spectral intensity and the spread of the distribution increase, reflecting enhanced energy deposition within the detector material. This behavior is consistent with the improved interaction probability of higher-energy photons in CdTe.

At lower energies (20–60 keV), the spectra appear weaker and less extended due to limited photon penetration and reduced energy transfer. In contrast, higher energies (80 and 100 keV) produce broader and more prominent spectral features, indicating more efficient detection and stronger signal generation.

Additionally, the absence of significant fluctuations in the simulated data highlights the idealized nature of the model, where electronic noise and charge collection losses are either minimized or not fully represented.

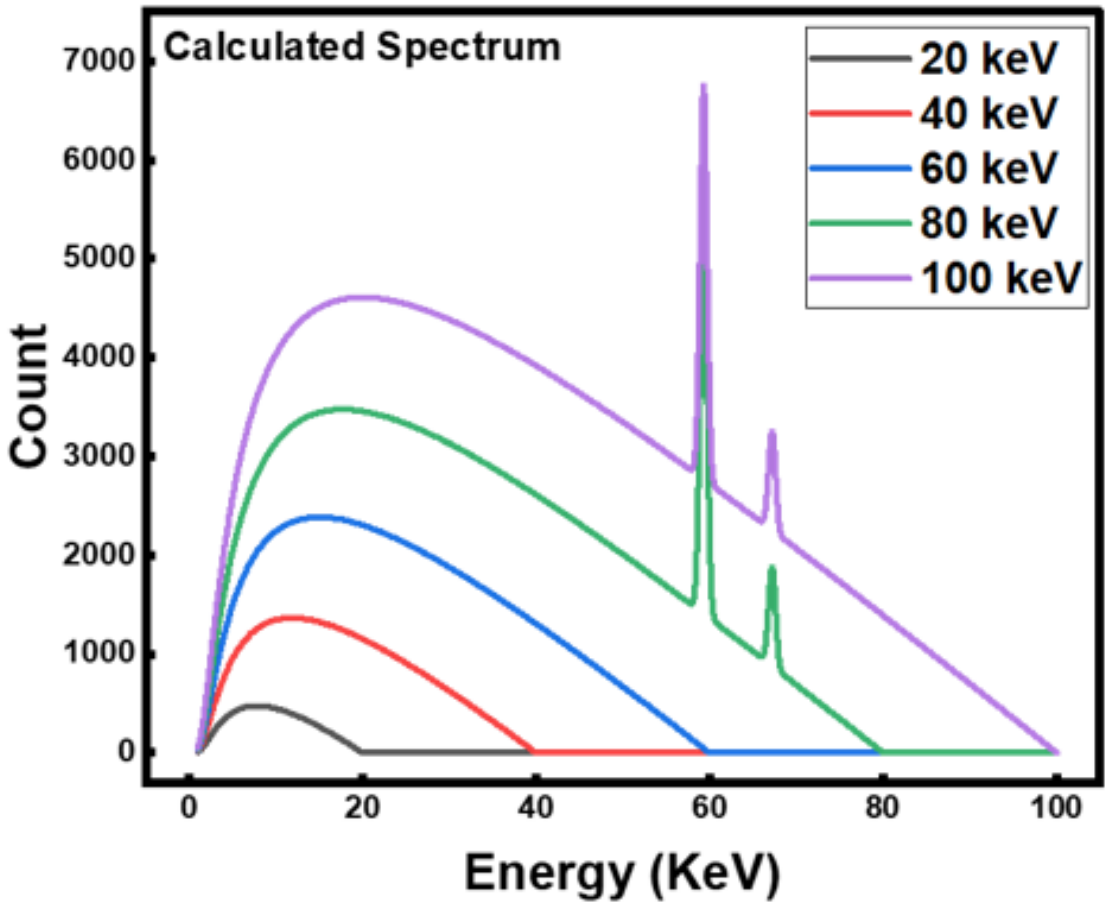

Fig.23: Simulated raw X-ray spectra for the CdTe detector at energies ranging from 20 keV to 100 keV, showing counts as a function of photon energy.

To enable a clearer comparison between different energies, the spectra were normalized to their respective maximum values. This normalization removes absolute intensity differences and emphasizes variations in spectral shape and distribution.

The normalized spectra reveal a consistent shift toward higher energies along with increasing spectral broadening. These trends reflect the dependence of detector response on incident photon energy and provide a clearer visualization of relative detector performance.

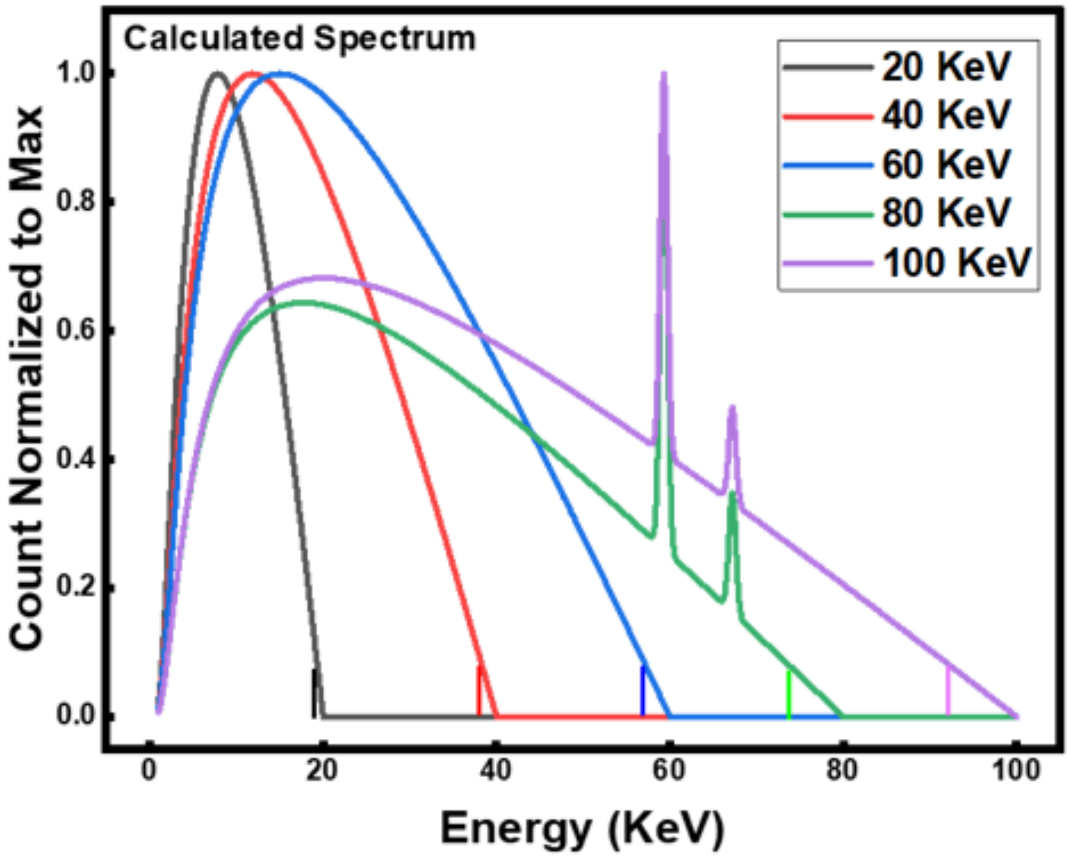

Fig.24: Normalized simulated X-ray spectra illustrating relative detector response across different photon energies.

Experimental Results

Experimental measurements were conducted under similar energy conditions to evaluate the real performance of the CdTe detector. Unlike the simulated results, the experimental spectra exhibit noticeable statistical fluctuations and noise.

The measured spectra show irregularities in peak shapes, particularly at lower energies, where the signal is significantly affected by electronic noise and limited energy deposition. In some cases, peaks are less distinguishable or appear broadened due to incomplete charge collection and detector resolution limitations.

At higher energies, the experimental spectra become more pronounced, with clearer features and improved signal definition. However, deviations from the ideal simulated behavior are still present, reflecting real-world effects such as air attenuation, electronic noise, and imperfections in the detector system.

These differences highlight the complexity of experimental measurements and the importance of accounting for non-ideal factors when analyzing detector performance.

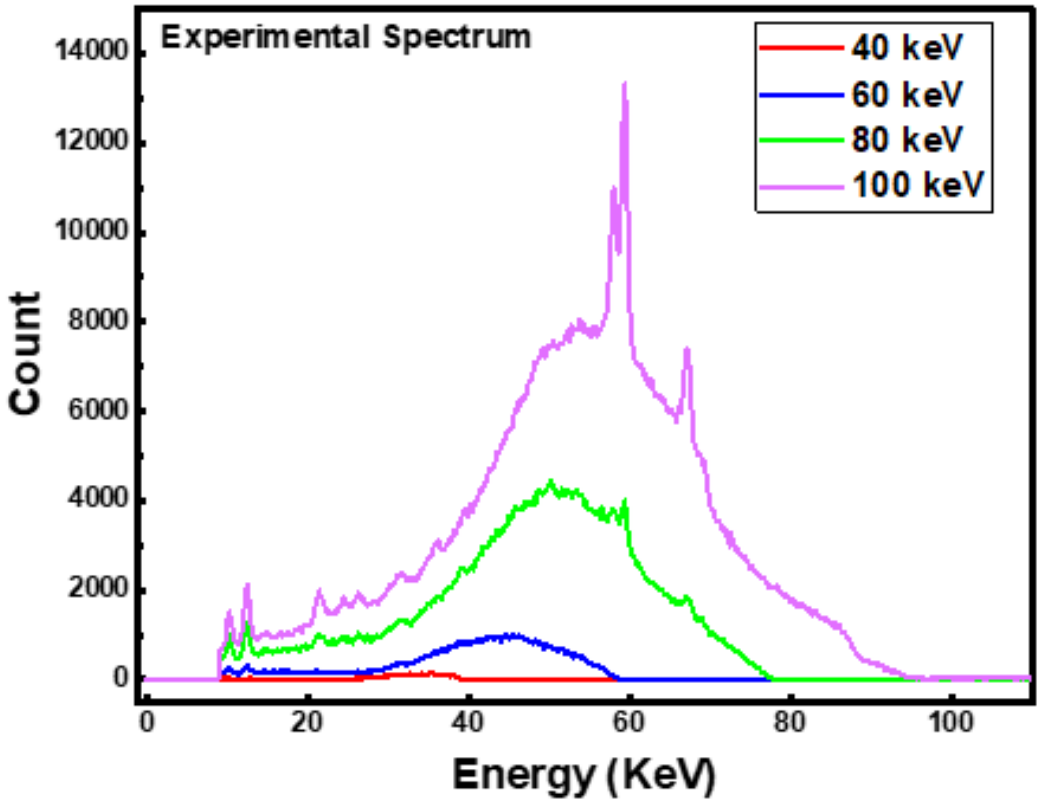

Fig.25: Experimental X-ray spectra measured using the CdTe detector, showing the effect of noise and detector imperfections on signal quality.

Similarly, the normalized experimental spectra provide a clearer comparison of spectral shapes. Despite normalization, fluctuations remain visible, emphasizing the stochastic nature of radiation detection and measurement uncertainties.

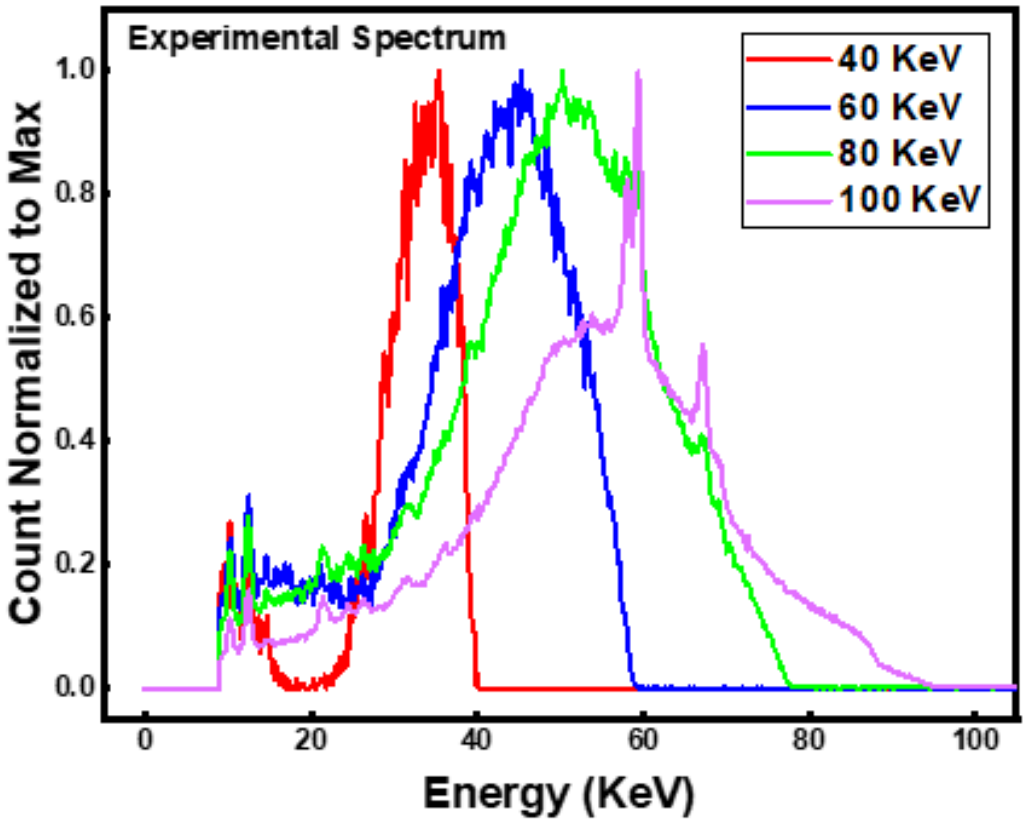

Fig.26: Normalized experimental spectra highlighting variations in detector response and the presence of statistical noise.

Comparison and Fitting Analysis

A direct comparison between simulated and experimental results was performed to evaluate the accuracy of the detector model. This comparison is illustrated using a fitting approach that correlates the applied X-ray tube voltage with the detected photon energy at 5% resolution.

The results demonstrate a strong linear relationship between the applied voltage and the detected energy, indicating good agreement between simulation and experimental measurements. This confirms that the simulation successfully captures the general behavior of the detector.

However, minor deviations between the two datasets are observed. These discrepancies can be attributed to several factors, including electronic noise, finite

energy resolution, charge collection inefficiencies, and uncertainties in experimental conditions such as alignment and calibration.

Overall, the fitting results validate the reliability of the simulation while also emphasizing the limitations inherent in practical measurements.

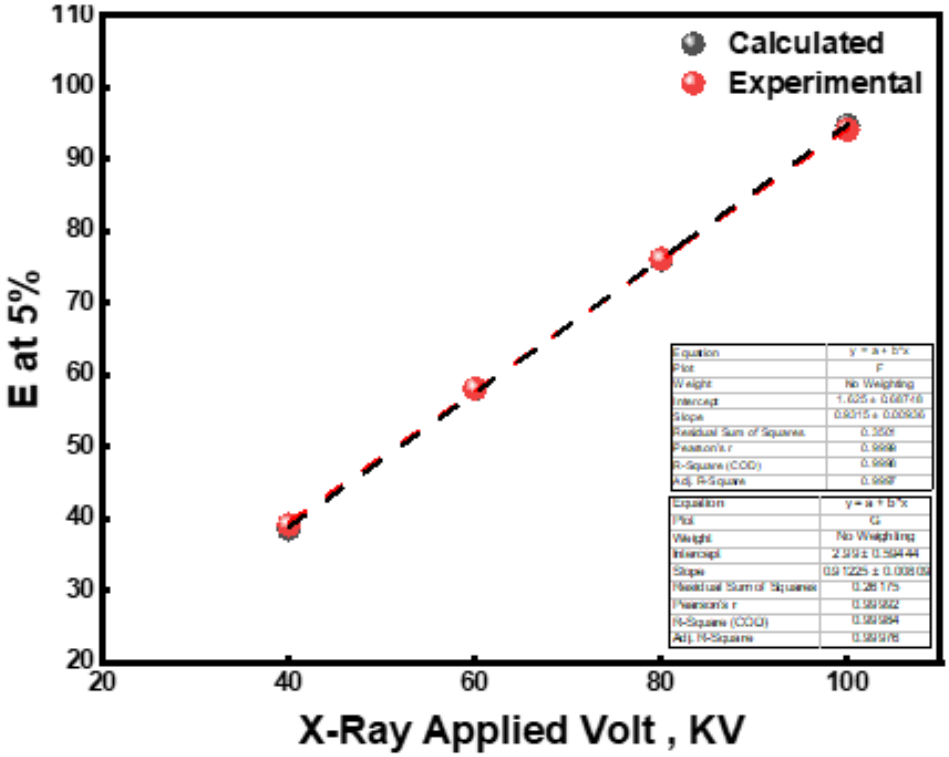

Fig.26: Comparison between simulated and experimental results showing the relationship between applied X-ray voltage and detected energy at 5% resolution.

The combined analysis of simulated and experimental X-ray spectra provides a comprehensive understanding of the CdTe detector performance. The simulation results offer insight into the ideal detector response, while the experimental data reveal the impact of real-world factors such as noise and detector inefficiencies.

The comparison and fitting analysis demonstrate strong agreement between both approaches, validating the simulation model and confirming its applicability for predicting detector behavior. These findings are essential for optimizing detector performance and improving the accuracy of X-ray spectroscopy measurements.

Conclusion

This study presents a comprehensive evaluation of different radiation detection systems, including semiconductor detectors (CdTe, Si, and GaAs) and scintillation detectors ($LaBr_3$ and BGO), for gamma-ray and alpha-particle measurements. The results demonstrate that detector material properties, such as density and atomic number, play a crucial role in determining detection efficiency, with CdTe exhibiting the highest performance among the investigated semiconductor detectors. The analysis of scintillation detectors shows that the energy resolution of $LaBr_3$ and BGO detectors improves with increasing applied voltage, primarily due to enhanced signal-to-noise ratio. This observation highlights the importance of carefully optimizing detector operating conditions to achieve high-precision gamma-ray spectroscopy.

In addition, the use of pixel detectors enabled the experimental determination of the alpha particle range in air, which was found to be consistent with Monte Carlo simulations performed using SRIM. The observed decrease in count rate with increasing distance confirms the expected energy loss mechanisms of alpha particles as they interact with air molecules, validating both the experimental approach and the simulation results. Furthermore, X-ray spectrum simulations conducted with the CdTe detector were compared with experimental measurements to validate the detector model. These simulations provided detailed insight into the detector response across different energy levels, showing that higher-energy photons are more efficiently detected and that optimized operating conditions substantially enhance detector performance and energy resolution.

Taken together, these results demonstrate that the combined use of experimental measurements and computational tools provides a robust framework for understanding radiation–matter interactions and improving detector performance. The comparative evaluation of different detector technologies also offers practical guidance for selecting suitable systems based on specific measurement requirements. Overall, this work emphasizes the critical importance of detector selection, calibration, and operating parameter optimization in achieving reliable and precise radiation measurements. These findings contribute to the development of more efficient and accurate detection systems and support ongoing advancements in nuclear physics, radiation monitoring, and applied scientific research.

Acknowledgement

I would like to express my sincere appreciation to my supervisor, **Prof. Dr. S. Abdelshakour**, for his continuous guidance, valuable insights, and unwavering support throughout the course of this work. His expertise and constructive feedback have played a fundamental role in shaping this research and improving its overall quality. I am also grateful to the **JINR START Programme team** for providing a stimulating research environment and for their cooperation and support during my participation in the program. Their efforts have greatly contributed to the successful completion of this work. My sincere thanks extend to my colleagues and mentors for their helpful discussions, encouragement, and continuous support. Their contributions were essential in overcoming challenges and refining the outcomes of this study. Finally, I deeply appreciate the opportunity to be part of this research experience, which has significantly enhanced my scientific knowledge, practical skills, and academic development. This experience has been invaluable in strengthening my interest in the field of radiation physics and its applications.

References

1. Persson, M., Wang, A., & Pelc, N. J. (2020). Detective quantum efficiency of photon-counting CdTe and Si detectors for computed tomography: a simulation study. Journal of Medical Imaging, 7(4), 1.
2. Si-PIN vs CdTe Comparison– Amptek – X-Ray Detectors and Electronics. (n.d.). Retrieved May 31, 2023
3. Schematic of a hybrid pixel detector with the sensor chip and the Download Scientific Diagram. (n.d.). Retrieved May 31, 2023
4. Poikela, T., Ballabriga, R., Buytaert, J., Llopart, X., Wong, W., Campbell, M., Wyllie, K., van Beuzekom, M., Schipper, J., Miryala, S., & Gromov, V. (2017). The VeloPix ASIC. Journal of Instrumentation, 12(1).
5. Knoll, G. F., Radiation detection and measurement, 4th Edition, Wiley (2010).
6. Martin J.E., Physics for Radiation Protection, WILEY-VCH Verlag GmbH & Co. KGaA, Weinheim (2013)
7. Knoll, G. F., Radiation detection and measurement, 4th Edition, Wiley (2010)